J. Fluid Mech. (1975), *vol.* 67, *part* 2, *pp.* 299–337
Printed in Great Britain

The vortex-street structure of 'turbulent' jets. Part 1

By J. C. LAU
University of Singapore
AND M. J. FISHER
Institute of Sound and Vibration Research, University of Southampton, England

(Received 11 March 1974)

It was suggested by Lau, Fisher & Fuchs (1972) that the basic structure of a 'turbulent' round jet might consist, essentially, of an axial array of fairly evenly spaced vortices moving downstream in the mixing region of the jet. The present experimental study is an attempt to establish this hypothesis on a sound footing. The problem which was posed was first to find proof of the existence of a fairly regular pattern in the mixing region, and second to extract detailed information on the component parts of this pattern to identify the nature of the structure.

Hot-wire signals in the mixing layer are known to possess a predominance of spikes. In the region closer to the high velocity side of the layer, these spikes tend to be downward ones whilst in the opposite region, they are upward. These spikes have been attributed to the entrainment mechanism in the mixing layer and had been thought to be random. A closer study of time-history curves of these hot-wire signals suggests that they might not be as random as would appear at first glance. A probability analysis was conducted of the time intervals between the successive downward spikes in the u' signals, and it was found that indeed the highest probability occurred when the time interval corresponded to a frequency equal to the vortex passing frequency.

A time-domain averaging (or eduction) technique was used to try to identify the nature of the flow structure using the spikes to trigger the eduction process. On the basis of these results it would seem that the suggestion of a vortex street is well founded. Furthermore, it appears that, as the individual vortices in the street move downstream, they are continuously transporting fluid masses across the mixing layer, and it is this effect which is producing the Reynolds stresses in the mixing layer, and causing the spikes in the u' signals in this region.

1. Introduction

1.1. *Background*

The structure of the 'turbulent' jet in the first few diameters has always attracted the attention of researchers. However, in recent times, the study of this structure has found renewed interest. This is due to two factors. The first is connected with the realization that, to obtain an explicit method of jet-noise prediction and, moreover, to establish an approach to the problem of jet-noise reduction on a less

ad hoc basis, it would be necessary first to understand the mechanism by which noise is generated in the jet. Such an understanding would come with a more definitive description of the jet structure.

The second factor is the recent discovery that the flow structure in the jet in these first few diameters (including the so-called turbulent mixing layer) is probably more regular and deterministic than had thitherto been thought possible. The evidence has suggested strongly that there may exist within the mixing layer of the jet a relatively regular pattern which is convecting downstream. Further evidence (Lau *et al.* 1972) has suggested the possibility that this regular pattern might have a controlling influence on the general flow field in the jet.

This has raised the hope that it may be possible to describe the jet structure in more explicit detail after all, and that with this detail the understanding of the noise-generating mechanism would follow. The present effort has therefore been directed towards obtaining a clearer picture of this regular pattern.

One of the earliest indications suggesting the possible existence of a regular flow pattern in the turbulent subsonic jet came from the work of Bradshaw, Ferriss & Johnson (1964). They carried out a survey in the general region of the potential core and the mixing layer situated in the first few diameters of the jet, and made measurements of various statistical properties in this region. They discovered that the spectra of hot-wire signals in the potential core had a narrow-band appearance. This result suggested that the fluctuations detected by the hot wire in the potential core were in fact the result of the passage of a fairly regular pattern. It was further argued that, as the major fluctuations in the jet were to be found in the mixing layer, the source of this regular pattern would most probably be situated in this layer.

Davies, Ko & Bose (1968) developed this concept of a convecting regular pattern in the jet, and undertook extensive hot-wire measurements in the potential core. They found that the convection velocity U_c was only about 0·65 of the local particle velocity (which incidentally was the jet efflux velocity U_0), and on the basis of their results of a probability density analysis of the signal, established that there was practically no probability of the signals detected in the potential core coming from a pattern moving with the local mean flow. On this line of reasoning, it seemed that the most likely location of the regular pattern would be the radial position in the jet where the local velocity was $0{\cdot}65U_0$. This location was found to be that of the region of maximum turbulence intensity. Moreover, it had been found earlier by Davies, Fisher & Barratt (1963) that the convection velocity at this location in the mixing layer was about $0{\cdot}65U_0$ also.

On the basis of this evidence, Davies *et al.* (1968) postulated that hidden in the general randomness of the flow in the mixing layer was in fact a regular pattern of 'sources'. As this pattern of sources convected downstream, it caused fluctuations to be generated in its vicinity, and it was these fluctuations which the hot wire detected in the potential core. They further showed, on the evidence of measurements of the convection velocity in the entrainment region of the jet, made by Franklin & Foxwell (1960) using microphones, that the influence of the source extended to the entrainment region also. Thus it would seem that this regular pattern had an influence on the flow field on both sides of the mixing layer.

The actual nature of the sources was however not known. One suggestion (Ko & Davies 1971) was that these sources were pressure-generating sources and that the hot-wire signals in the potential core were actually manifestations of the pressure fluctuations.

1.2. *The basic vortex model*

An effort was therefore made to identify the nature of the regular pattern. Drawing on the supposition that the signals in the potential core and the entrainment region were the manifestations of the same flow field, which had its origin in the mixing region, Lau *et al.* (1972) carried out a series of correlation measurements of the fluctuating pressure p' and the axial and radial velocities u' and v' in the potential core and the entrainment region. From the phase relationships of p', u' and v' derived from these correlation results, they obtained a picture of the regular pattern. The picture consisted essentially of an axial array of discrete vortices spaced about one and a quarter nozzle diameters apart. This they designated as the 'basic vortex model'. This array of vortices was assumed to convect downstream in the region of maximum turbulence at a speed of $0{\cdot}65U_0$. As the array moved downstream, it caused fluctuations in its vicinity. Since the jet was round, it was assumed that the vortices would be toroidal in shape.

There has been ample evidence in visualization pictures of round-jet flows in which a toroidal-vortex pattern exists at low Reynolds numbers (e.g. Anderson 1956). The correlation results would seem to suggest that this vortex pattern was preserved to some extent even in the high Reynolds number cases (i.e. well after turbulence had apparently set in). The question remained, nevertheless, of the extent to which this 'basic vortex model' would account for the observed flow characteristics in the mixing layer of a fully turbulent jet.

Two difficulties were immediately apparent. First, if the pattern is as regular as suggested by observations in the jet potential core and entrainment region, why do fluctuations observed in the mixing layer have a relatively random appearance? It was felt (Lau *et al.* 1972) that this could be explained on the assumption that successive vortices did not follow precisely identical paths. Far from the vortex cores (i.e. in the jet potential core and entrainment region) these differences would have little effect on the observed signal, creating perhaps some degree of amplitude modulation only. Conversely, close to the vortex cores (i.e. in the mixing region), these differences in path would cause different cross-sections of successive vortices to 'cut through' the hot wire thus yielding differing signatures and giving a generally more random appearance to the hot-wire signal.

A far more serious objection, however, was that the 'basic vortex model' failed completely to predict the existence of any mean Reynolds shear stress in the jet mixing layer. This problem has been discussed previously in Lau *et al.* (1972) and an extension to the basic model as proposed therein, which does provide a mean Reynolds stress. The purpose of this paper is to provide additional confirmation for that model using data eduction techniques, in contrast to the correlation approach used previously.

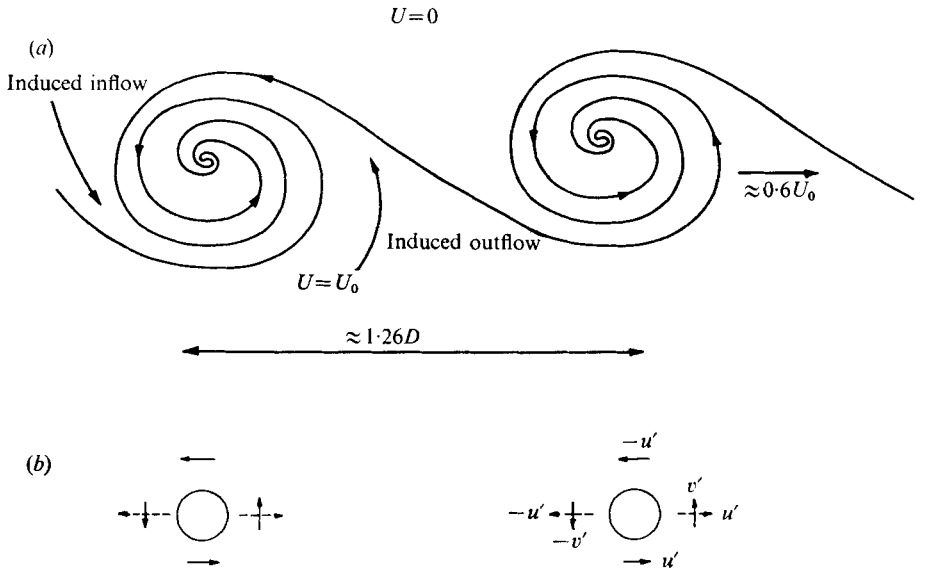

FIGURE 1. Extended vortex model. (*a*) Pictorial representation. (*b*) Induced velocities: ——, due to basic vortex; – – –, due to nonlinear mass transfer.

1.3. *The model of 'turbulent' jet structure*

A sketch of the extended vortex model is shown in figure 1. In common with the 'basic vortex model' it still comprises primary vortices in the mixing layer spaced one and a quarter nozzle diameters apart and being convected downstream at about 0·65 times the nozzle efflux velocity. It is hypothesized in addition, however, that the leading edge of each vortex induces an outflow of high velocity fluid from the potential-core side of the mixing region across into the low velocity region. By the same token relatively low velocity fluid is transported radially inwards towards the potential core by the trailing edge of each vortex. It is an examination of the evidence for this hypothesis which forms the basis of the present study.

The mechanism proposed would have the effect that an observer stationed in the outer part of the mixing layer would see a sudden increase in the axial flow going past him every time that a vortex passes. In the inner part of the mixing layer he would observe a sudden drop in the axial flow with the passage of a vortex.

Referring to figure 1 (*b*), it may be seen that, under the influence of each basic primary vortex, the induced velocities orientate around the vortex core. These velocities are shown by the full arrows in the figure. As a result of the mechanism just described, other velocity perturbations would also be set up alongside, and these are shown by the broken arrows. In such a case, it can be seen that a positive u' signal would correspond to the appearance of a positive v' signal, and a negative u' to a negative v' signal. The net effect is that a non-zero.mean value of $u'v'$ would occur wherever the cross-flow is significant, which might explain the presence of Reynolds stresses in the jet.

Some justification for the extended model may be found in correlation results

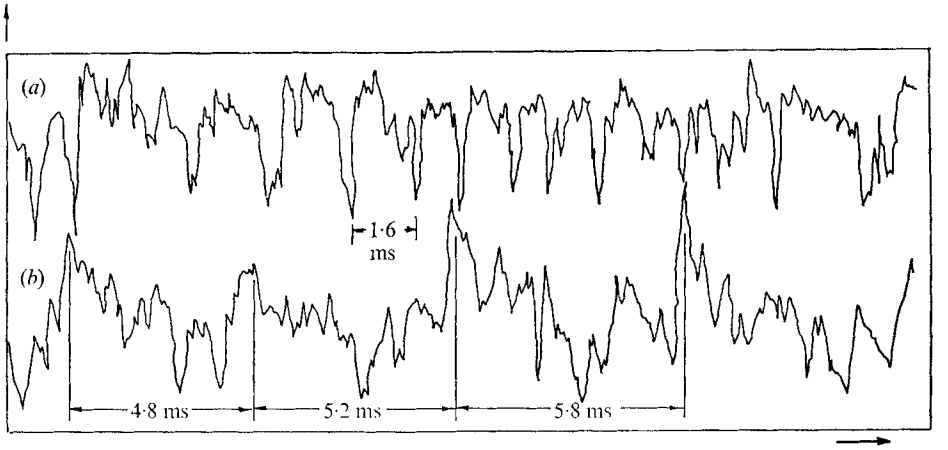

FIGURE 2. Time-history traces of hot-wire signals obtained at (*a*) $r/D = 0{\cdot}4$ and (*b*) $r/D = 0{\cdot}6$ within the mixing layer of the jet. $x/D = 2{\cdot}0$.

within the mixing region (Lau *et al.* 1972). However, a more interesting and revealing result of the effect of this cross-flow mechanism may be obtained from the time-history traces of the u' signals in the mixing layer.

The suggestion of the extended model is that a burst or spike would be registered every time that a primary vortex goes past a hot wire placed in the mixing layer. With the hot wire placed on the entrainment-region side of the vortex core, the spike would be an upward one; and on the potential-core side, a downward one. With this in mind, the spikes in long time-history traces of the u' signals may be studied in detail.

Figure 2 shows the simultaneous time-history curves of u' signals on either side of the path of the vortex cores. The top trace is for the case when the hot wire was at the radial position $r/D = 0{\cdot}4$, and the lower for $r/D = 0{\cdot}6$. The spikes may be seen very clearly in both the traces.

At the jet speed at which these traces were taken, the time interval between succeeding vortices was expected to be about 1·6 ms. It may be seen in the upper trace that, although the spikes do not fall after precisely this interval every time, there is a tendency for the intervals between spikes to lie close to this value.

The intervals between the upward spikes of the lower trace are not as well defined. In fact, the lower trace raised some questions because the intervals between the extremely large upward spikes appear to be about three times longer (i.e. the frequency of these extremely large spikes appears to be about one-third of the vortex passing frequency). A plausible reason for this will be given in part 2. It should be pointed out at this juncture, however, that these extremely large upward spikes in each case appear at instants very close to those at which the downward spikes appear in the upper trace, thus suggesting that the large upward spikes could be related to the passing of the vortices.

1.4. *The present study*

The relatively good correlation between the predictions of the extended vortex model and experimental results, particularly with respect to the downward

spikes, gave impetus to the present work. The aim was to try to establish this model of 'turbulent' jet structure on a firmer basis. As a first effort, the intervals between the downward spikes were statistically analysed. This allowed the evaluation of the most probable frequency of occurrence of the spikes. This phase of the work will be reported in §3. The spikes were next used as the triggers in a time-domain averaging (or 'eduction') process. By means of this technique, only the signal information which is associated with the events causing the spikes is retained whilst all extraneous information is averaged out. The results of this work will be presented in §4. An explanation of the eduction technique will appear in §2.

2. Experimental set-up and techniques

2.1. *The air supply*

A 5·08 cm circular nozzle was used. This nozzle diameter was large enough to allow fairly good resolution of the jet field and yet did not put an overly heavy demand on the air supply. It was also thought worthwhile to obtain data on a nozzle for which far-field noise measurements were available. A fuller description of the air system appears in the paper by Lau *et al.* (1972).

The experiments were conducted at a speed of 61 m/s. At this speed, the jet had all the characteristics of a 'turbulent jet'. As the fluctuations were Strouhal-number dependent, it was decided to restrict the tests in this report to this one speed.

2.2. *Standard instruments*

Hot wires and microphones were used to measure velocity and pressure fluctuations in this study. A description of these instruments and a full assessment of their use appeared in an earlier paper (Lau *et al.* 1972). Correlation results were obtained using the technique which was also described in that paper.

2.3. *Spike converter*

The spike converter was designed specifically to study the spikes. It converts the successive intervals between the spikes in the u' signals into a series of sawtooth voltage ramps. Figure 3 shows a block diagram of the instrument.

Each ramp is initiated when the input signal voltage exceeds a predetermined value. Therefore, as the voltage of each spike in the hot-wire signal passes this set value, a ramp will be started. Provision is available in the instrument for adjusting the triggering voltage level (Lau 1971).

Since the slope of the ramps is constant, the maximum voltages attained by the ramps gives a direct measure of the intervals between the spikes. An example of the output ramps of the spike converter appears in figure 4. The corresponding input signal is shown below. A sketch appearing at the bottom of the figure shows how the ramps may be interpreted. It may be seen that the output ramps reach saturation on some occasions. This will occur when the time between one spike and the next becomes too large. In the mode in which the instrument was used during the investigation saturation occurred at a voltage corresponding to a time interval of 3·33 ms.

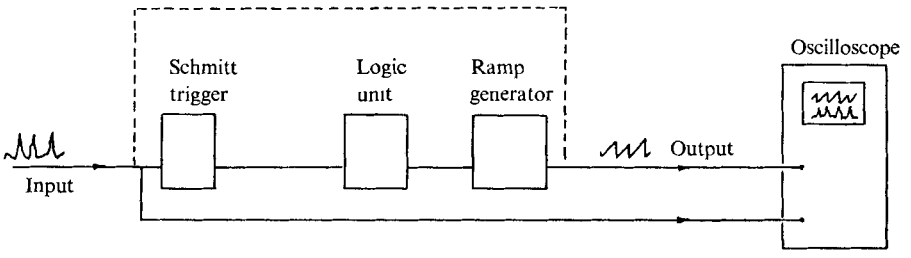

FIGURE 3. Block diagram of spike converter.

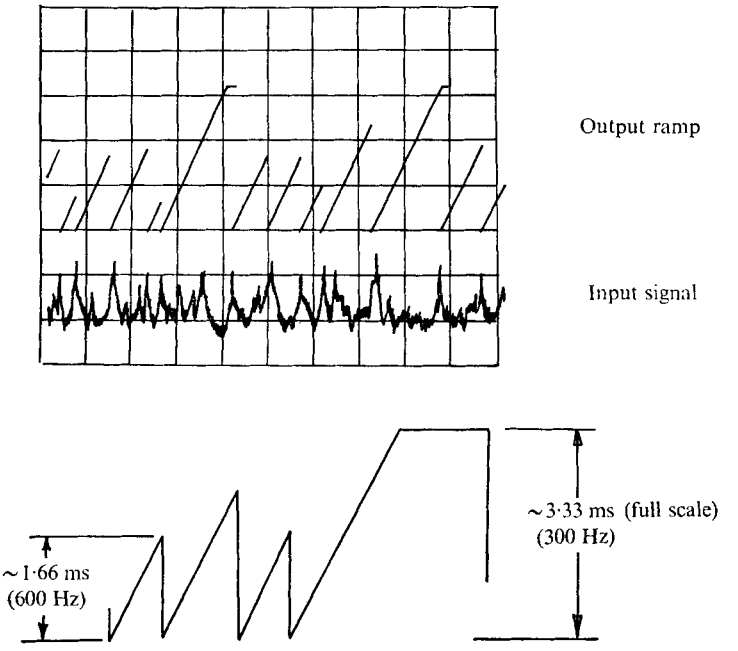

FIGURE 4. Output ramp of spike converter.

2.4. *Time-domain averaging (or eduction) technique*

A Hewlet-Packard Model 3721A correlator was used for this work. Although the usual function of this instrument is as a correlator, it possesses also an option which allows it to recover repetitive signal components from a general signal.

The instrument conducts a simultaneous computation of the ensemble averages and the results are displayed as a function of time. The length of the time domain displayed may be varied in the range 100 μs–100 s. The output from the spike converter was used to trigger the eduction process. For these tests the results were displayed on an X–Y plotter.

A fuller description of this technique and the results from it have already been documented (Lau 1971). However, a brief review of the theory behind the technique and its uses may be appropriate at this point.

In order to demonstrate the principle behind the technique, we shall quote

the example of research into the physiological responses of animals subjected to a given stimulus. It is in this area that the technique finds its most frequent and longstanding application. This example also permits a more vivid description of the technique. When an animal subject is given a particular stimulus, it will react immediately in response. Under the usual environmental influence, a portion of the reaction would be as a direct consequence of this stimulus, but the rest of the reaction might be spurious and totally unconnected. One important aspect about this unrelated or spurious response is that, if an ensemble of these responses were taken and averaged, the result would be a consistent zero response throughout. Therefore, in an attempt to isolate and recover fully the responses which are directly related to the application of the stimulus, many identical stimuli would be applied to the subject under similar conditions, and the realization of its reactions averaged. This would result in the spurious information averaging out to zero, leaving the directly related information behind.

This may be illustrated mathematically as follows. If the total response is given by $A(t)+B(t)$, where $A(t)$ represents the response which is related to the stimulus and $B(t)$ the spurious response, then a sample of the realizations of the total response from many stimuli may be given by

$$\begin{aligned}
&A(t_1)+B_1(t_1), \quad A(t_2)+B_1(t_2), \quad A(t_3)+B_1(t_3), \ldots,\\
&A(t_1)+B_2(t_1), \quad A(t_2)+B_2(t_2), \quad A(t_3)+B_2(t_3) \ldots,\\
&\vdots\\
&A(t_1)+B_N(t_1), \quad A(t_2)+B_N(t_2), \quad A(t_3)+B_N(t_3), \ldots,
\end{aligned}$$

where t_1, t_2, etc., represent instants in time following the application of the stimulus. It should be noted that $A(t)$ remains unchanged from one realization to the other since the same stimulus is applied in each case.

The ensemble of realizations may then be averaged to give

$$\frac{1}{N}\sum_{k=1}^{N} A(t_1)+B_k(t_1), \quad \frac{1}{N}\sum_{k=1}^{N} A(t_2)+B_k(t_2), \ldots .$$

If N is large enough,

$$\frac{1}{N}\sum_{k=1}^{N} B(t)$$

should tend to zero for all t, and since

$$\sum_{k=1}^{N} A(t) = NA(t),$$

the result of this averaging process would produce

$$A(t_1), \quad A(t_2), \quad A(t_3), \ldots,$$

which is a sample of the responses of the subject that are directly caused by the stimulus.

It is obvious from this that, the greater the number of realizations taken in the averaging, the more representative the result will be. However, there is a limit to the advantage that can be gained in each case by increasing this number of realizations. The limiting number would depend on the proportion of spurious signal contained in the overall response. In an experimental procedure, the

technique would be to increase gradually the number of realizations taken until the moment was reached when any further increase in the number of realizations would not give any improvement in the results.

The next point to note is that, for the proper working of the technique, it is not necessary for the stimuli to be applied at regular intervals. The only prerequisite is that they should be identical in each case.

In the example quoted, the instant at which the stimulus is applied offers a suitable reference time with which to align all the response histories. However, there is no reason why any point in the response history may not be used as this reference time, provided that (*a*) this point has a unique position with respect to the response related to the stimulus, and (*b*) it has features which stand out and make it distinguishable from the rest of the signal. For the work described here, the downward and upward spikes in the u' signal were used as the stimulus to initiate the eduction.

3. The interval between the spikes in u' signals

In order to determine the most probable period between the downward spikes, a special computer program was written. This exercise was designed to produce a distribution of the probability of these periods falling between certain times. If the spikes were indeed as regular as suggested, the distribution would show a peak value corresponding to the most probable period. This value could then be used to determine the most probable frequency of occurrence of the spikes.

The spike converter was used for this study. Figure 5 shows how the signals were processed through the spike converter to produce the ramps and how the ramp voltages were sampled. The hot-wire signals with downward spikes were first fed into a signal inverter which transformed the original signal to one with a series of upward spikes. This inverted signal was then fed to the Schmitt trigger Unit within the spike converter, which initiated a voltage pulse every time that the voltage of the input signal exceeded a preset threshold level. These pulses were then used to activate the ramp generator. The ramps which were generated were next fed to a Marconi Myriad II computer for processing.

The computer program operated using the following procedure. First, the voltage ramps were sampled at regular small intervals ΔT, as shown in figure 5. Each sampled voltage was then compared with the previous one, and the difference ascertained. If the later sample had a higher voltage than the earlier one, this meant that the two samples had been taken on the rising part of the ramp. However, when the succeeding sample voltage was lower than the previous one, this signified that a point had been reached when a new ramp was being generated. By keeping account of the number of samples taken between each successive new ramp, the intervals of the ramps were determined. These intervals were statistically analysed to give a probability distribution.

Figures 6 (*a*)–(*c*) show the probability distributions of the ramp durations: the ordinate gives the probability of ramps with durations falling within each of the equal time bands shown on the abscissa. For the data shown about 2900 ramps were processed. These diagrams show the results obtained when the triggering

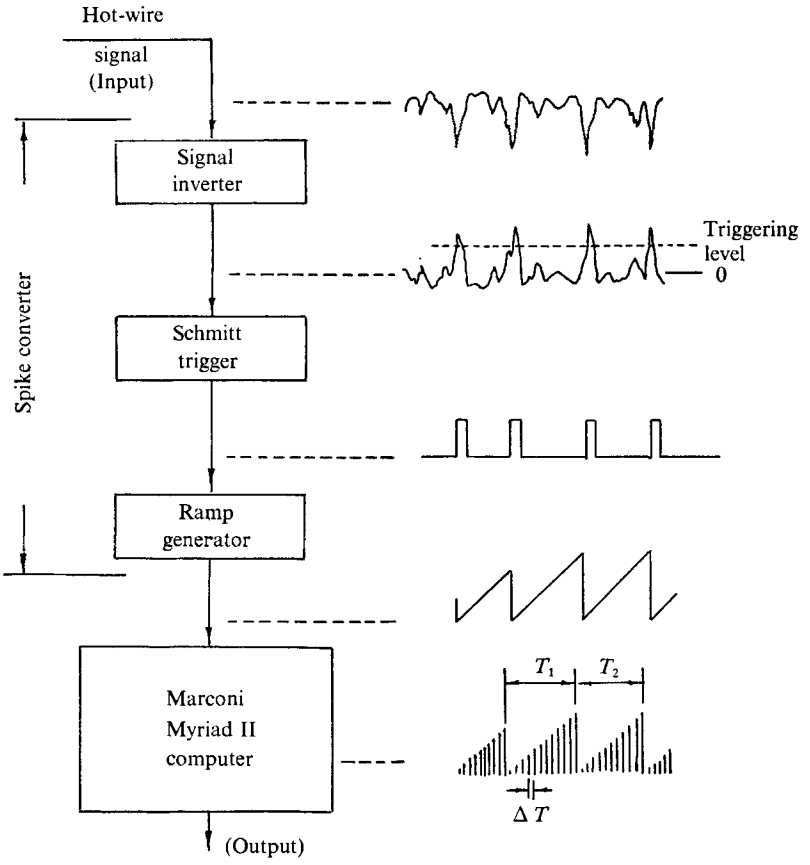

FIGURE 5. Flow diagram of spike signals.

level is set at progressively lower negative voltages (at $-0{\cdot}59$, $-0{\cdot}49$ and $-0{\cdot}39$ V). It may be seen that, in the first case, the highest probability appears in the time band between 1·55 and 1·75 ms, whilst in the latter two cases it is between 1·40 and 1·60 ms. It would appear, therefore, on the basis of the overlapping times that the most probable duration of the ramps lies in the region of 1·55 ms. This would correspond to a frequency of 640 Hz, which would compare well with the proposed vortex passing frequency of 620 Hz.

It would seem, therefore, that there is some connexion between the downward spikes in the u' signals within the mixing region and the passage of the vortices. However, whilst there appears to be a maximum probability of the spike frequency at the proposed vortex passing frequency, it may be seen that, as a percentage of the total, the probability is relatively low. Moreover, there is almost as high a probability at time intervals on either side of this maximum.

It may be seen, for instance, from figure 6 (*a*) that, even at a time interval of about 3·25 ms, the probability is still about half the maximum value. The relatively high probability at such long times may be explained by the fact that, at this triggering level, many of the spikes have been missed. Evidence of this

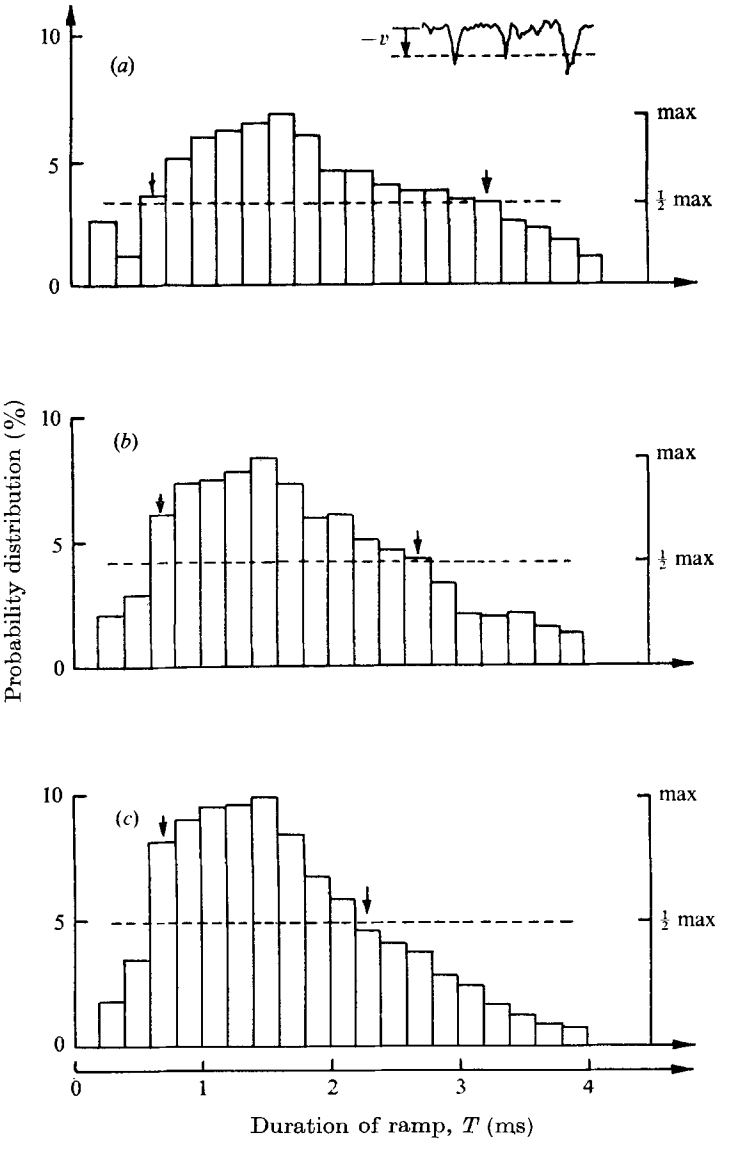

FIGURE 6. Probability distributions of duration of ramps. Triggering voltage: (*a*) −0·59 V, (*b*) −0·49 V, (*c*) −0·39 V.

was seen in the oscilloscope trace of the signals and the ramps during the experiment. This possibility may perhaps be better appreciated if we look at the other two diagrams, where it may be seen that the probability falls to half of the respective maximum values at intervals of about 2·7 ms and 2·3 ms respectively. In these latter diagrams, because the triggering levels are brought closer to the signals, fewer of the peaks are missed.

Whilst lowering the magnitude of the threshold level has the effect of including more of the spikes, it also brings in the possibility of the ramps being initiated by

the underlying irregularities in the signal. This could explain the tendency for the probabilities at lower times to rise with decreasing negative triggering voltage. This may be seen more clearly in the rise of the probability level at around 0·7 ms, say, in figures 6 (*a*)–(*c*).

On the whole, it would seem, therefore, that the spikes were indeed connected with the passage of the vortices, except that the vortices were not passing in as regular and orderly a manner as an idealized model of exactly evenly spaced vortices might suggest.

4. The eduction results

4.1. *Introduction*

In the present investigation into the flow structure of the jet, the assumption of the model, developed on the basis of the experimental evidence, is that an all-pervading regular pattern exists in the flow regime covered by the first few diameters of the jet. It is further suggested that the steady convection of an array of almost identical and fairly evenly spaced vortices is the underlying structure causing the regular pattern. Therefore, a repeatable pattern is expected to be observed every time that one of the vortices of the array passes the observation point. There is some hint of such an almost repeatable and regular pattern in the measurements in the potential core and the entrainment region. However, in the mixing region it has been more difficult to detect. In fact, as was found in the preceding section, although there is a higher probability of an almost repeatable pattern recurring at a given frequency, its recurrence is not always precisely after the same interval. Moreover, time-history curves do not show identical patterns around each spike.

The poorer definition of the pattern in the mixing region seems to be due to small random excursions of the pattern from its mean form and the likelihood that there is a cross-current of fluid in the mixing region caused by nonlinear effects. For instance, it appears that the vortices may not be exactly the same distance apart at all times and that they do not all move along a definite path. These excursions could cause very drastic changes in the signals observed by a fixed instrument placed in this region. This therefore makes it impossible to obtain meaningful information about the structure of the jet merely by direct transposition from the time-history curves. Clearly, therefore, to identify fully the structure of the jet, other techniques will have to be sought, and it was for this purpose that the eduction technique was developed and employed. Since the spikes in the u' signals appear to be associated with the passage of vortices, they became the logical choice for the data for triggering the eduction process.

4.2. *Details concerning the spikes*

A study of the way the spikes develop might be useful at this juncture. For this purpose, it is proposed to consider the development of the spikes for the two cases shown in figure 7.

The case of a hot wire placed at $r/D = 0{\cdot}4$. In this case, the hot wire is situated on the potential-core side of the vortex street. In the basic vortex model, where

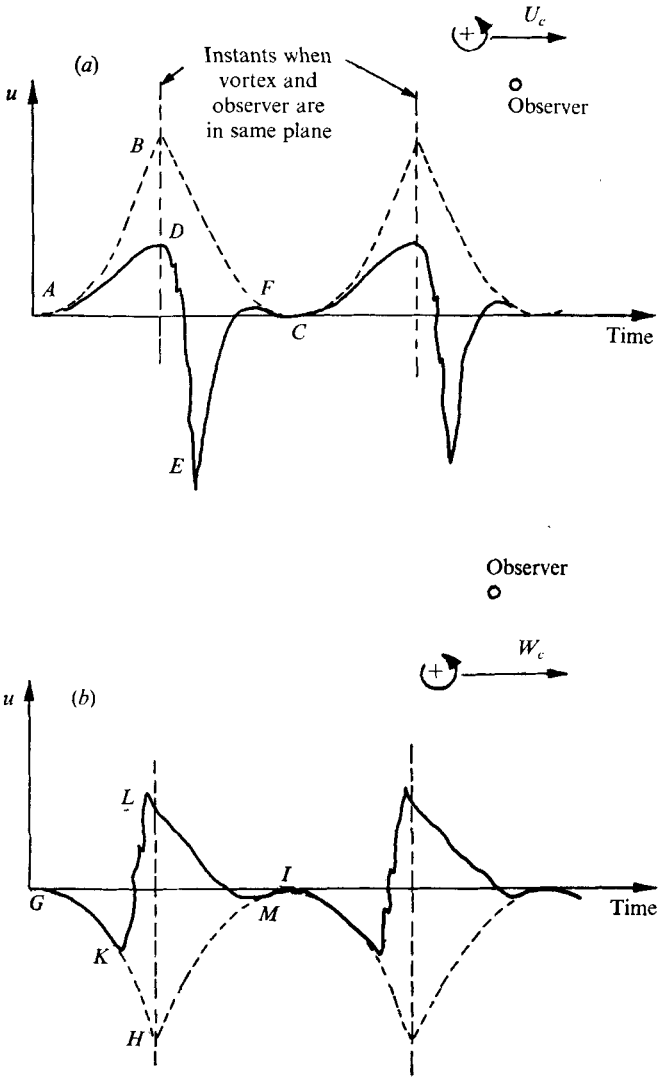

FIGURE 7. Sketch showing the development of spikes in u' signals. (*a*) $r/D = 0{\cdot}4$. (*b*) $r/D = 0{\cdot}6$.

the convection of the array of vortices is the only mechanism and no mixing is involved, the signals experienced by the observer (hot wire) at this position follow the path traced out by ABC in figure 7. The observer experiences a rise in the u-component signal as the vortex approaches. This will be followed by a similar fall as the vortex recedes from him. However, when secondary effects come into play, and some of the high velocity fluid on his side of the shear layer is first thrown radially outwards away from him, he experiences changes along a new path AD. As the vortex begins to move past him, its trailing edge sweeps slugs of low velocity fluid from the other side of the shear layer. This latter movement of fluid has a more positive effect, and is manifested in a sudden drop in the

value of the u-component velocity. This sudden drop is indicated by DE. Instead of a smooth drop along DE, there are most probably a number of little dips due to the very nature of the mixing process, and the fact that fluid being convected across the mixing layer may contain concentrations of little 'satellite' vortices. The fall persists until secondary flow is no longer significant. At this time, the flow reverts to the 'clean' flow condition traced out by EF and continues on to C, at which time the process repeats itself.

The case of a hot wire placed at $r/D = 0{\cdot}6$. This case is somewhat different from the above because the first experience of the observer with the approach of the vortex is bursts of high velocity fluid being thrown at him by the leading edge of the vortex. Therefore, instead of following the path indicated by GH, the trace reflects the influence of the bursts and goes along GKL instead. As the vortex centre passes the observer, fluid is drawn away from the observer, and the trace gradually drops, finally returning to the 'clean' flow curve HI at M.

From this explanation, it would appear that the upward spikes (i.e. at $r/D = 0{\cdot}6$) in general precede the downward spikes (i.e. the trace at $r/D = 0{\cdot}4$). Figure 2 seems to show some support for this. The very large upward spikes do appear in general to occur at an instant just before the downward ones.

4.3. *Panoramic view of the extended model of jet structure*

Having established some idea as to how the spikes might be generated, it would be interesting now to review the main points of the extended model and draw some conclusions on the kind of results which one might expect from the eduction process.

The essence of the model is shown in figure 8. In this figure, only three of the whole array of vortices are shown, and they are supposed to be convected from right to left. Therefore, to a stationary observer, the fluctuations induced by this movement of the vortices would appear to vary, the time axis running from left to right as in the diagram. It should be noted that the vortices would be spaced about $1{\cdot}3D$ apart.

The vortices are assumed to induce a cross-flow of fluid from one side of the mixing region to the other. Therefore, an observer on the inner side of the region experiences a sharp drop in velocity whenever the trailing edge of the vortex comes in line because low velocity fluid from the outer side of the region is brought to him. In a similar manner, an observer on the outer side experiences a sudden increase in velocity when the leading edge of the vortex comes in line. In the context of the model, these surges would appear as large downward and upward spikes in the detected signals. The approximate positions of these spikes are shown in the middle of the figure.

This transverse movement of fluid is assumed to influence the conditions in the mixing region only where there is non-uniformity in the mean flow. Therefore, in the potential core and the entrainment region, it is expected that the fluctuations remain mostly unaffected by any cross-flow, and depend solely on the passing of the primary vortices. In this case, the anticipated u' signals and p' signals for these two regions would be as shown in the figure. It may be noted that they have a practically sinusoidal appearance, the pressures in the two

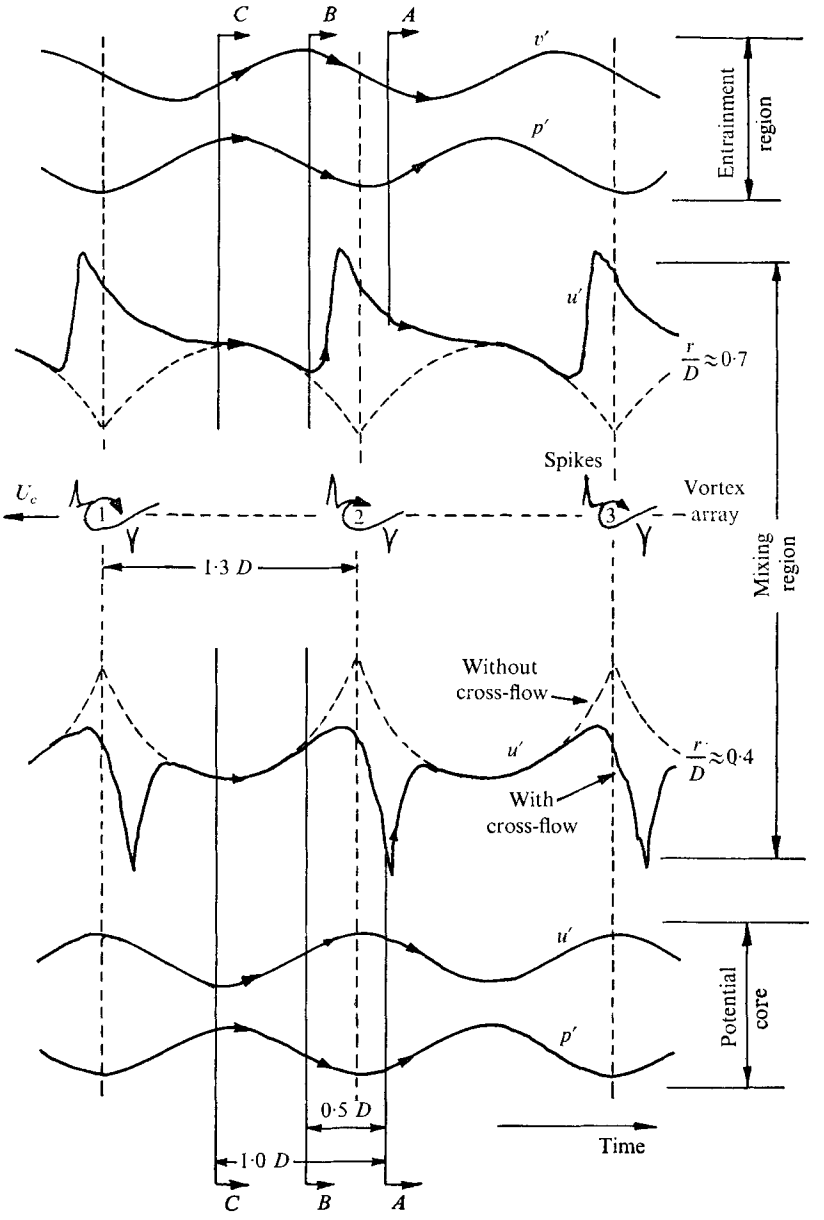

FIGURE 8. Flow field derived from the extended model of jet structure.

regions being in phase, and the u' signals in antiphase. This in essence is what was established prior to the extension of the basic concept of the model.

In the mixing region, however, the cross-flow would be expected to make some modifications to the signals detected. It is not possible to predict what the effect on the pressure signals of this modification would be, but, as will be seen, there does not appear to be any significant effect at all. With the v' signals, however, it is expected by reason of the mechanism of the cross-flow that the form and

phase of the signal would remain essentially unchanged, although there might be changes in the amplitude.

The signals which would be most greatly affected would be the u' signals. This was considered at length in §4.2, and on the basis of that discussion, projected wave forms of the modified u' signals for the mixing region have been derived and are shown in the figure. It may be seen that the whole character of the u' signals is changed as a result of the cross-flow, and consequently the upward and downward spikes are generated. It should be noted that the downward spikes occur a short time after the passing of the vortex centre whilst the upward spikes precede the vortex centre by a similar amount.

The curves presented in this figure, therefore, give a picture of the field that may be expected from the flow structure postulated in the extended model. Let us therefore try to predict the forms of the signals which might be expected to be recovered by the eduction technique. Since downward spikes are used to trigger the eduction, the actual instants of triggering would in general occur somewhere along the downward slope of the spikes.

For the sake of the present argument, we shall assume that the spike of vortex 2 initiates the eduction of a typical realization, and that the recovery probe is a microphone placed in the potential-core region. For this case, the signals of the recovery microphone will only begin to be registered after the spike of vortex 2 reaches the hot wire whose signal is used to trigger the eduction. If the recovery microphone is at the same axial station as the triggering hot wire, it is expected that the recovered signal will begin at the point designated by A and proceed to the right along the p' curve for the potential core. However, if the recovery microphone is at some position downstream from the triggering hot wire, $0{\cdot}5D$ downstream, say, the recovered signal will begin to be registered at an earlier stage on the curve, at B in fact. The further downstream the recovery microphone is placed, therefore, the earlier will the curve of the recovered signal begin. With the recovery microphone at yet another downstream position, $1{\cdot}0D$, say, the curve will commence at C. Thus, if the recovery microphone is moved downstream in steps, the origin of the recovered signal will move to the left of the curve, so that a given peak in the curve will appear to occur at increasing times. From these remarks, it is clear, therefore, that in order to reveal more of vortex 2, the vortex immediately connected with the triggering spike, the recovery microphone will have to be placed at least $0{\cdot}5D$ downstream of the triggering hot wire.

The whole argument may be extended to the signals at other radial positions in the field, and applied to other components of the fluctuations as well.

4.4. *Measurements in the potential core*

In order to test the system and to assess the validity of the assumption about the use of the technique, measurements were made in the potential core. The choice of this particular region to test the technique was dictated by the fact that the first and strongest indications of the possible existence of the regular pattern in the jet field have been in this region. Moreover, the signals detected in this region have been found to have a consistent appearance similar to that predicted by the model. Thus a clear assessment of the technique would be possible merely by

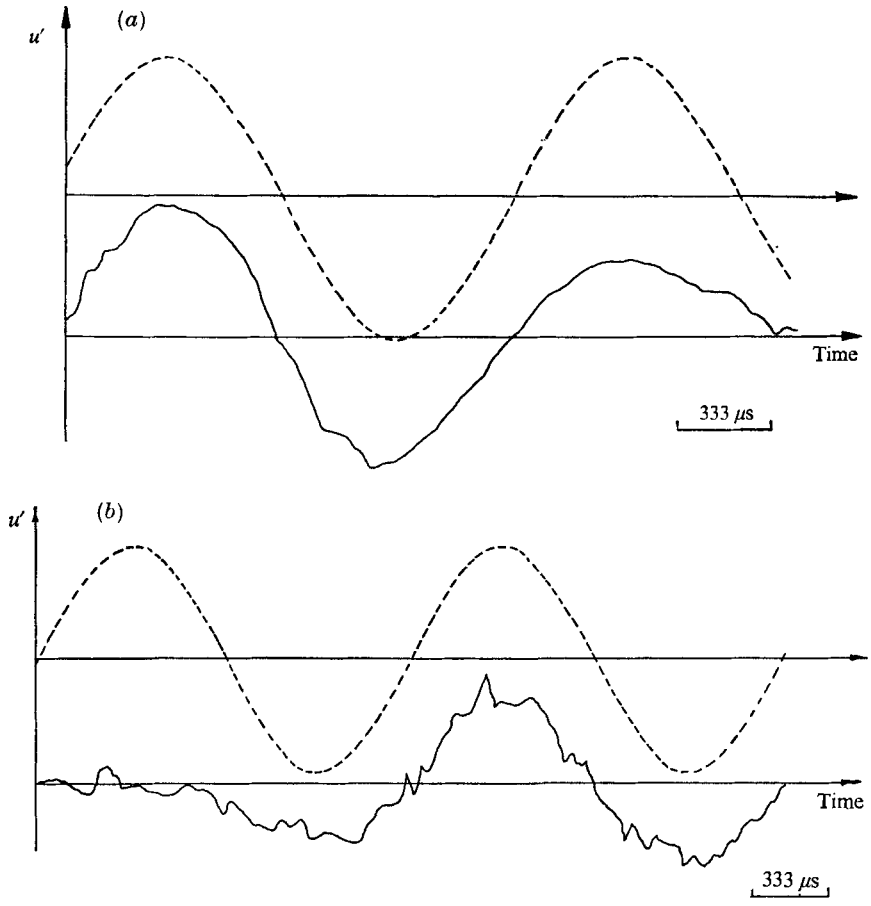

FIGURE 9. Comparison of predicted and educed u' signals on the jet axis. ——, predicted; – – –, educed. (*a*) Recovery hot wire positioned $0{\cdot}5D$ downstream of triggering hot wire. (*b*) Recovery hot wire $2{\cdot}0D$ downstream of triggering hot wire.

juxtaposing the results of the eduction technique and a trace of the predicted signal.

Figure 9 (*a*) shows such a comparison between the predicted and an actually educed signal at the jet axis. For this case the recovery hot wire was placed $0{\cdot}5D$ downstream of the triggering hot wire, which, in terms of the field shown in figure 8 for the model, represents the case of the observer at B. It may be seen that, in the main, the educed signal follows very closely the form of the predicted curve. The phase relationships are generally reproduced, and the two curves oscillate nearly sinusoidally about the zero level with frequencies of the same order.

The only significant difference between the two curves is that, whilst the predicted curve oscillates at a constant amplitude, the educed curve appears to be damped. It is clear that the diminishing amplitude is not due to the varying amplitude of the original signal as the averaging process would even it out. It suggests, in fact, that the vortices are not very consistently spaced. It is therefore

expected that the amplitudes of the signals will not be as well recovered if they happen to be associated with vortices which are at some distance from the one triggering the eduction. This is illustrated in figure 9 (*b*), which shows the recovered signal at a point $2{\cdot}0D$ downstream of the triggering hot wire. It may be seen that on either side of the high peak the amplitude of the signal falls. This peak is directly associated with the actual vortex triggering the eduction. Therefore, only the influence of the vortices close to the ones triggering the eduction is expected to be recovered.

It may further be noted that the curves of figures 9 (*a*) and (*b*) represent signals educed at two points which are about one vortex spacing apart. The fluctuations should therefore have a phase separation of almost one wavelength. This may be seen to be the case. Thus, it appears that information on relative phases may also be recovered by the technique.

The generally good agreement between the phases of the recovered and predicted signals might also be taken to suggest that the spikes are connected with the vortices as previously supposed. Moreover, it justifies earlier assumptions that the spikes appear in the wakes of the vortices. Thus meaningful conclusions about the relative phases of various component fluctuations may be inferred from the recovered signals.

It therefore appears that the system using the downward spikes to trigger the eduction is a practicable and functional one, and may be used with confidence to reveal the elementary structure of the regular pattern in the rest of the flow field.

More hot-wire measurements. Figure 10 shows more extensively the results of the eduction of hot-wire signals in the potential core. The triggering hot wire was placed at $x/D = 2{\cdot}0$, $r/D = 0{\cdot}4$. The results u'_R were obtained with the recovery hot wire placed on the jet axis and each curve represents the educed signal at a particular axial position of this probe with respect to the triggering hot wire. The separation is designated by ξ. For clarity, only portions of the curves are shown except for the case $\xi/D = 2{\cdot}0$.

It may be seen clearly from the portions of the curves shown that the recovered signals have a nearly sinusoidal appearance. It may also be seen from the full curve shown for $\xi/D = 2{\cdot}0$ that the recovered signal does not persist beyond one and a half wavelengths at most. As was suggested earlier, this is due to inconsistencies in the spacings of the vortices.

It is significant that the signals are recovered fairly well at downstream positions also. This suggests that the vortices are convected at a fairly consistent speed because, if this were not the case, the recovered signal here would drop significantly. Therefore, it would appear that the irregular intervals between the spikes observed in the time-history curves might be due more to inconsistencies in the spacing of the vortices than to irregular convection velocities. It is also significant that the peaks of the recovered signals occur later and later as the recovery hot wire is moved downstream. This is consistent with what was predicted earlier from the model and suggests that the convection velocity may be determined from the family of curves, in much the same manner as space–time correlation curves have been used before. In fact, values of the convection

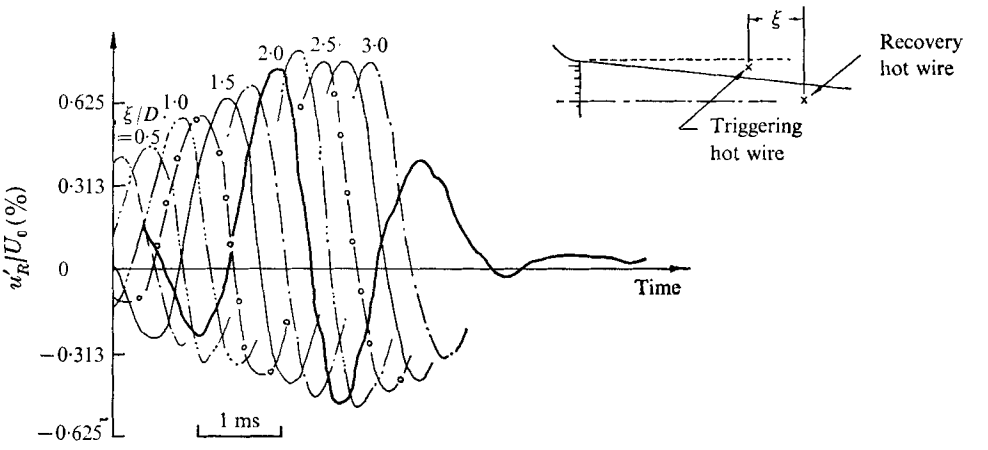

FIGURE 10. Recovered hot-wire signals for jet axis. Triggering hot wire at $x/D = 2{\cdot}0$, $r/D = 0{\cdot}4$.

velocity were determined from the curves and found to range from 0·64 at $x/D = 2{\cdot}0$ to about 0·76 beyond $x/D = 3{\cdot}0$. These are identical to the results obtained by standard correlation techniques (Lau 1971).

It may be seen from figure 10 that the magnitudes of the peaks in each curve grow with axial distance downstream, thus suggesting that the influence of the vortex system on the jet axis increases with downstream distance. This conforms with other results which show that the intensity of axial velocity fluctuations increases with increasing axial distance from the nozzle (Fuchs 1970; Lau 1971). An explanation for this will appear in part 2. However, a comparison of the two results would be useful and they are plotted in figure 11 alongside each other.

It may be seen that both curves rise monotonically. The ratios of the peak amplitudes of the recovered signals to the corresponding r.m.s. values of the original signal were computed and their distribution is shown in the figure. It may be seen that the ratio appears to stay at a constant value of about 0·23. This ratio of the recovered signal might appear at first glance to be very low. However, on further consideration and in view of what has been said about the very restrictive requirements of the eduction process, the inconsistent nature of the spikes and even of the signals in the potential core themselves, such a low magnitude should not be altogether surprising. After all, the spikes do not have a consistent shape and size although they may herald the vortices faithfully. Thus the physical instants when the eduction is triggered may not be precisely the same each time. Since the proportion of the signals recovered seems to be constant along the jet axis, and as the signals in the potential core have a more consistent appearance, this ratio may be used as the norm for the proportion of the signals likely to be recovered throughout this investigation.

Finally, the first curve suggests a periodicity that leads to a frequency of about 620 Hz. The spectral peak frequency for the axial positions shown ranges from about 640 to about 510. Thus the results follow the model quite faithfully.

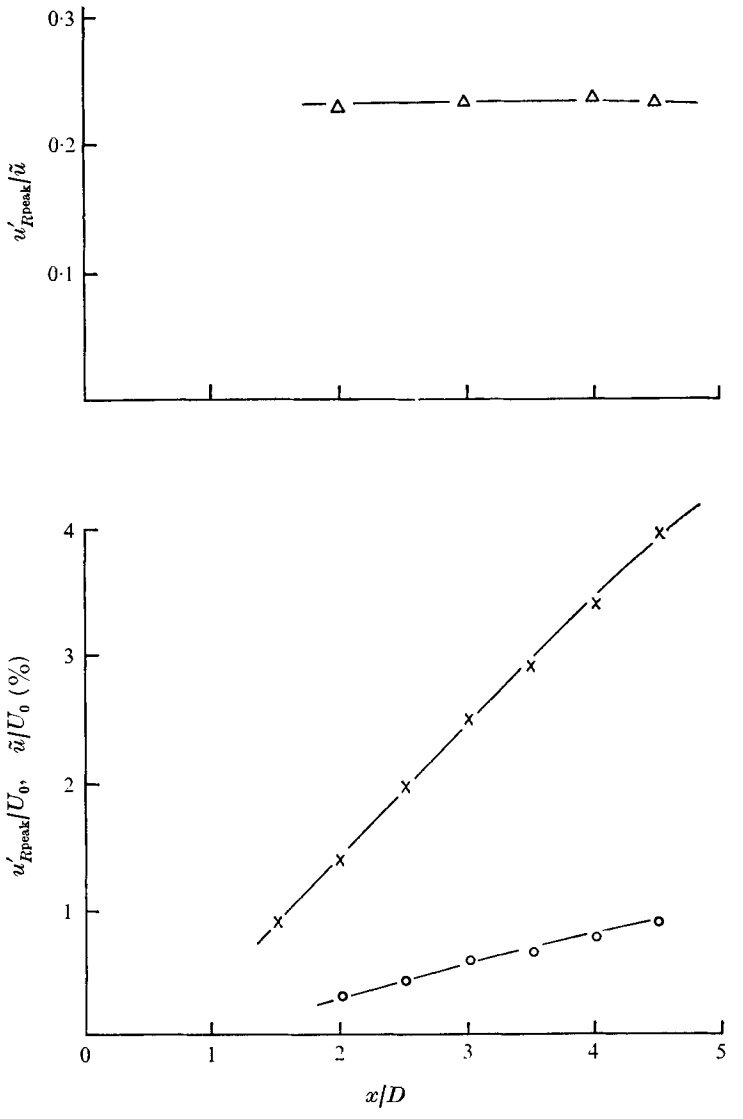

FIGURE 11. Comparison between peak amplitude of recovered signals and the r.m.s. intensity $\tilde{u}$ of fluctuations along the jet axis. ○, $u'_{R\text{peak}}/U_0$; ×, $\tilde{u}/U_0$.

Microphone measurements. Figure 12 shows results of the microphone measurements along the jet axis. The triggering system was the same as before. It may be seen that the shape of the curves is quite similar to that of corresponding curves of hot-wire signals. Once again, only about one and a half wavelengths of the history are recovered, thus reinforcing the point made earlier that the vortices are not always an exactly constant distance apart. Approximately the same proportion of the original signal was recovered, and the values of the convection velocity and frequency of oscillation of the curves were found to be of the same orders of magnitude as above.

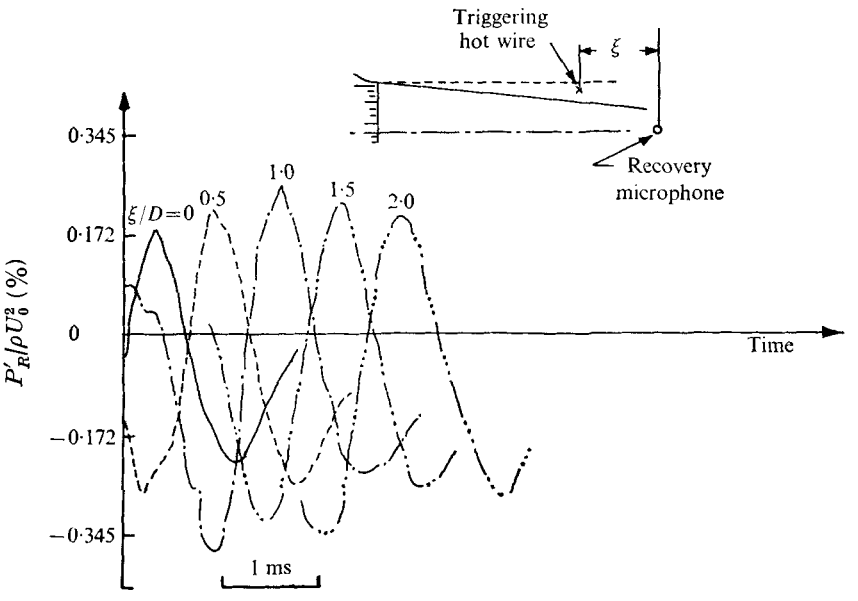

FIGURE 12. Recovered microphone signals along jet axis.

Considering the curve for the case when the sensitive point on the microphone is in line with the triggering hot wire (i.e. $\xi/D = 0$), it may be seen that it begins at a very small negative value, proceeding to a positive value, and then goes to a first positive turning point. Reference to figure 8 will show that these trends follow the predictions of the model for an observer at A. Comparison of the trends for other positions of the microphone will lead to the same conclusion.

Thus the pressure results also faithfully follow the predictions of the model.

4.5. *Measurements in the entrainment region*

The entrainment region is the other region where evidence of the regular pattern has been found. It is therefore appropriate that results for this region receive our attention next.

Hot-wire measurements. Figure 13 shows the recovered signals for $r/D = 1{\cdot}1$. A normal hot wire was used for this purpose. The hot wire was orientated perpendicular to the radial and the axial flow. Since it was found (Lau 1971) that the mean flow was directed radially inwards at this radial position, the velocity recovered is more akin to v'. It does seem though that for more accurate amplitude measurements a cross-wire probe should be used. However, for the present survey, since we were mainly interested in phase relationships, it was felt that use of a single-wire probe was justified.

It was found that the amplitude of the recovered signal was about a third of the r.m.s. value of the signal. This ratio compares well with those determined for the potential core, and indicates that the eduction is meaningful for this configuration.

The curves have a jagged appearance suggesting that the signals are unstable.

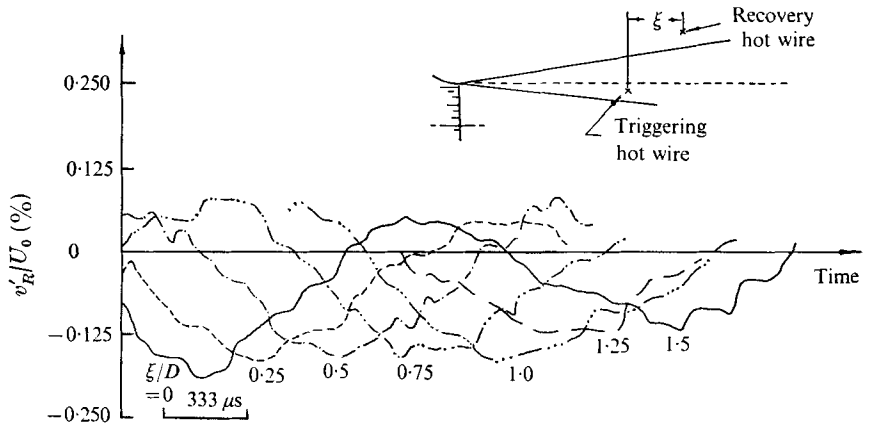

FIGURE 13. Recovered hot-wire signals for $r/D = 1{\cdot}1$.

This is understandable since the mean velocity here is very low and therefore the flow is greatly influenced by even the slightest room draughts. However, in spite of the jaggedness, it was possible to obtain an estimate of the average frequency of oscillation of the curves and the convection velocity. These turned out to be about 580 Hz and $0{\cdot}69U_0$ respectively, which are of the same orders of magnitude as the values found in the potential core.

Assuming that the educed signal represented the v' fluctuations as suggested, let us now consider in some detail the curve for $\xi/D = 0$. For this case, the curve begins at a negative value and continues to a negative peak value. The first turning point is therefore a negative peak. Referring to the top trace of figure 8, it may be seen that this is the trend predicted by the model for the recovery hot wire positioned at A. A similar observation may be made for the other curves also.

Microphone measurements. The recovered microphone signals for $r/D = 1{\cdot}1$ are shown in figure 14. Only three curves are shown. It may be seen that the jaggedness noticed in the hot-wire signals is not present. As for the curves obtained in the potential core, only about one and a half wavelengths of the history are recovered. One outstanding feature is the high proportion of the signal recovered. About four-ninths of the r.m.s. value of the signal was recovered as compared with about one-quarter in the potential core. This was not altogether to be expected in view of the recovery probe being further away from the triggering hot wire and perhaps reflects the greater efficiency of the microphone in a quiescent region such as the entrainment region rather than that of the technique.

The curves may be seen to have the same phase relationships as corresponding ones in the potential core and to be in agreement with the model. The frequency of oscillation and the convection velocity are in exact agreement with measurements made in the potential core also.

In summary, therefore, the results of this subsection have shown once again that earlier comments about the technique and the likely position of the spikes relative to the vortices are well founded. This would suggest that full confidence may be placed in the ability of the technique to reveal the basic structure of the regular pattern in the mixing region.

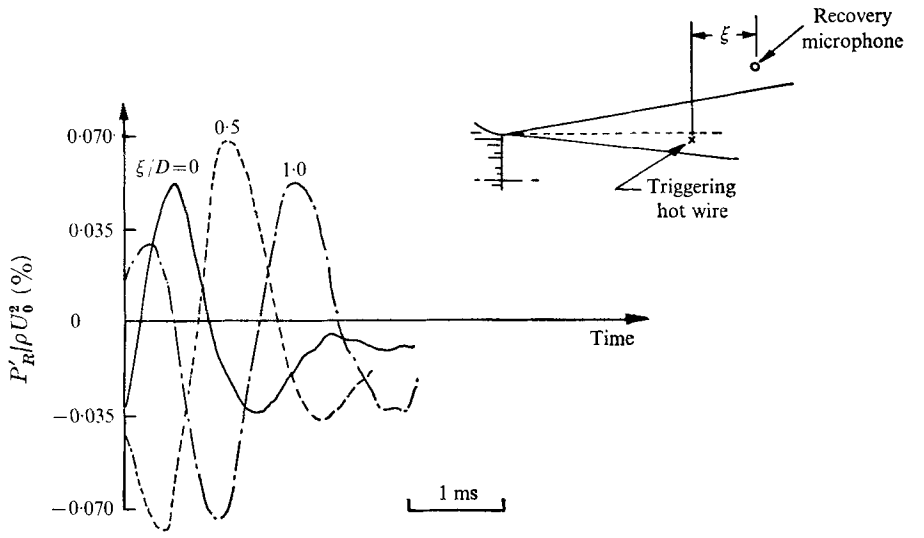

FIGURE 14. Recovered microphone signals for $r/D = 1{\cdot}1$.

4.6. *Measurements in the mixing region*

From the two previous subsections, it would seem that the system for the eduction of the regular pattern using as the trigger the downward spikes of the u' signals in the mixing region is viable. With this assurance, measurements were made in the mixing region, where some doubt has been entertained concerning the existence of such a regular pattern. In particular, we were interested in trying to recover signals within the mixing region which might reveal the existence of the regular pattern there.

As in earlier cases, the triggering hot wire was placed at the position $x/D = 2{\cdot}0$, $r/D = 0{\cdot}4$.

Hot-wire measurements. Figure 15 shows the signals recovered for $r/D = 0{\cdot}5$. It may be seen that the curve representing the case when the recovery hot wire is in line with the triggering hot wire ($\xi = 0$) begins at a negative value and proceeds to a negative peak. After the peak, the curve appears to rise gradually until the positive peak. For the case $\xi/D = 0{\cdot}5$ on the other hand, the curve begins at a positive value and proceeds gradually to a negative peak. These two curves may be seen to be almost in antiphase, which is understandable since they represent observations made at two points which are nearly half a vortex spacing apart. Moreover, if the characteristic shapes and the phases shown by these curves are compared with the predictions given in figure 8, it will be seen that the details suggested are quite in harmony with the predictions of the extended model. Thus it appears that the signal that is recovered is associated with the cross-flow as indicated by the model.

It may be seen that the peak values of the recovered signals fall very quickly with increasing ξ. On the other hand, it has been found (e.g. Bradshaw *et al.* 1964) that the r.m.s. values of the signals remain essentially constant at the positions for which the curves of figure 15 were recovered. When the recovery hot wire is

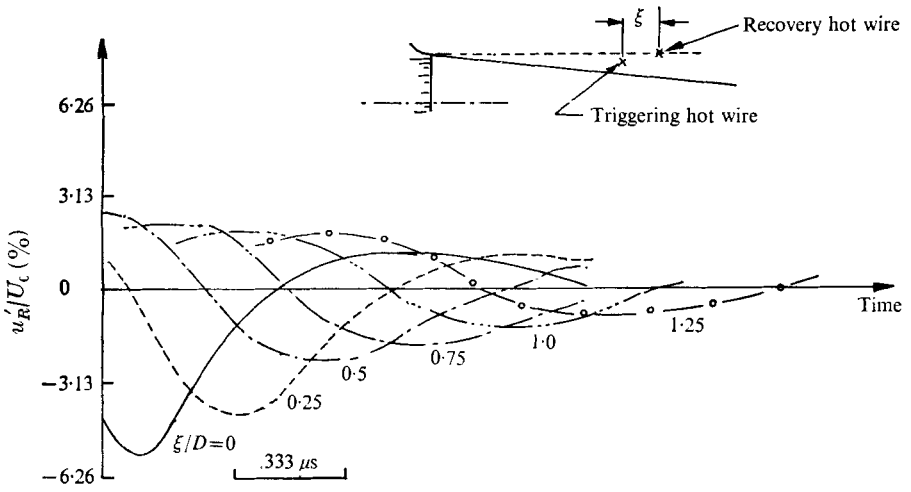

FIGURE 15. Recovered hot-wire signals for $r/D = 0{\cdot}5$.

close to the triggering hot wire ($\xi = 0$) the recovered signal is about half the r.m.s. value. This is higher than the ratio of 0·23 for signals recovered in the potential core. However, as the recovery hot wire is brought downstream, the proportion falls to about one-eighth. If, as was suggested earlier, the proportion 0·23 is taken as the norm for what one might expect to recover with nearly constant amplitude signals like those in the potential core, the higher ratio of the recoverable peak value to the r.m.s. value would merely suggest that spikes are occurring in the signals and that they can be fairly well recovered. The fact that this proportion could fall within about half a diameter to values below the norm for nearly constant amplitude signals would suggest that the spikes are not very well preserved as they move downstream and that the cross-flow causing the spikes is essentially a localized phenomenon.

However, in spite of this last point, it seems clear that the cross-flow generally exists within the framework of a nearly regular pattern. This may be seen from the fact that the curves do show some oscillation about the zero level and have a periodicity which is of the same order of magnitude as that of the proposed vortices. Furthermore, meaningful recovery can be obtained as far as one and a quarter diameters downstream of the triggering hot wire (i.e. at $x/D = 3{\cdot}25$). It would appear, therefore, that, although the cross-flows have a somewhat localized character, they are in the main formed around the vortex pattern.

Partly to verify this hypothesis, signals were recovered at a fixed point in the flow field at three speeds. The results are shown in figure 16. It may be seen that, as the speed is decreased, the curves expand along the time axis whilst keeping essentially the same general shape. The times of the zero crossings are also shown, and it may be seen that they are inversely proportional to the jet speed. Thus, the concept of the cross-flows being bound to the vortices of the regular patterns seems feasible.

The convection velocity of the signals was determined from the family of

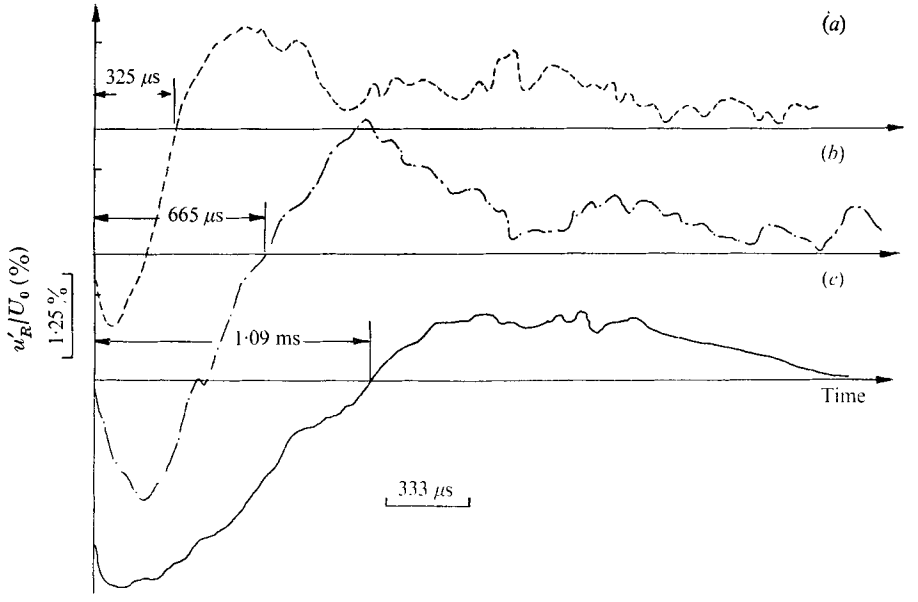

FIGURE 16. Effect of jet velocity on recovered hot-wire signals for $x/D = 2{\cdot}0$, $r/D = 0{\cdot}5$. (*a*) $U_0 = 91$ m/s. (*b*) $U_0 = 61$ m/s. (*c*) $U_0 = 30{\cdot}5$ m/s.

curves to be $0{\cdot}63U_0$. The corresponding value from correlations was $0{\cdot}66U_0$. The fact that a convection velocity which agrees with that found by other techniques can be determined from these curves at all is of some significance. It suggests that the components contributing to the localized fluctuations caused by the cross-flow still form a dominant part of the flow at the downstream position, and more significantly, that they have nearly the same relative phase relationship with the vortices at the downstream position as upstream. The implication may be that some of these fluctuations continue to be bound to the primary vortices as they are convected downstream.

It appears, therefore, from the foregoing that there is some sound basis for the concept of vortices continuously transporting fluid across the mixing region as they move downstream as suggested by the model.

Figure 17 shows the signals recovered for $r/D = 0{\cdot}6$. It may be seen that the recovered signal does not decay with downstream displacement of the recovery hot wire as in the previous case, but by the same token, the magnitudes of the recovered signals in the initial positions do not reach such high values either. This is understandable since the eduction is now carried out at a relatively larger radial distance from the triggering point, and emphasizes the point made earlier about the localized nature of the cross-flow.

The phase relationships of the curves may again be shown to follow the predicted curves.

The curves may be seen to oscillate, as in all the previous cases, about the zero level. However, the frequency of the fluctuations is less than 500 Hz. This value is lower than one might expect from the vortex model, but is higher than the value 300 Hz, which is the approximate frequency determined from the peaks

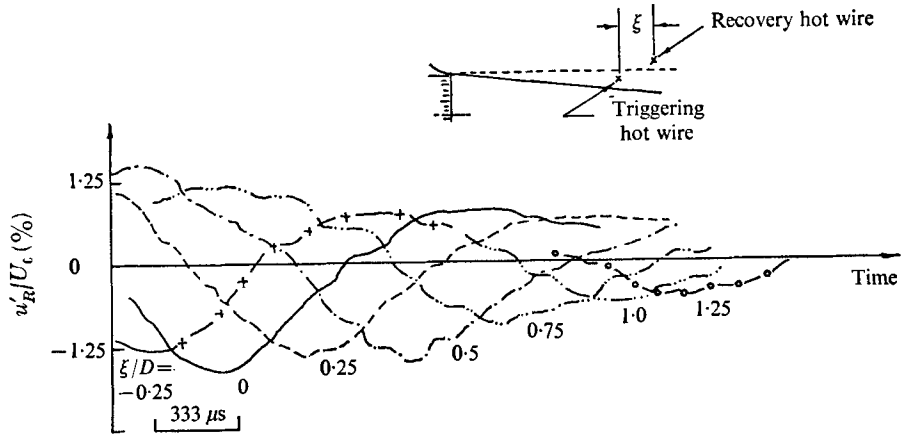

FIGURE 17. Recovered hot-wire signals for $r/D = 0{\cdot}6$.

of the hot-wire spectra at this point. The reason why the frequency of oscillation of the recovered signal is less than the vortex passing frequency and indeed why the spectral peak frequency is still less is not immediately obvious, but conceivably it could be tied up with the mechanism which caused the upward spikes here to appear at about one-third of the vortex passing frequency. However, as will be seen, the results in §4.7 do suggest the possibility of a second flow component in this outer region, and it seems possible that the recovered signals here are influenced by this second component.

As in the previous case, the convection velocity of the recovered signal was determined from the family of curves. This was found to be about $0{\cdot}63U_0$, exactly the same as that found at $r/D = 0{\cdot}5$. Therefore, it appears that, in this region also, the localized cross-flow fluctuations recovered are bound to the vortices. This is especially meaningful since the mean velocity at this point is equal to $0{\cdot}33U_0$. Therefore, there seems to be little doubt that the cross-flows are carried with the vortex system and not the mean flow. This underlines also the belief that only the effects associated with the vortices are recovered.

Figure 18 shows the signals recovered for $r/D = 0{\cdot}7$. It may be seen that the proportion of the signal recovered is much less than that found so far. This is understandable as the flow here seems to be under the influence of factors other than the primary vortex system. However, the shapes and the origin of the curves still seem to follow the model predictions fairly closely and a convection velocity of $0{\cdot}58U_0$ could be obtained. It may be seen, however, that this value of the convection velocity is lower than those found earlier at other radial positions.

It may be seen, therefore, that the velocity results recovered, particularly on the inner side of the mixing region, follow very closely the predictions of the extended model. The phase relationship, the frequency of oscillation of the recovered signals and the derived values of the convection velocity are seen to duplicate the predictions faithfully.

On the outer side of the mixing region, however, the agreement is not as good. For instance, the frequency of oscillation of the signals was found to be lower

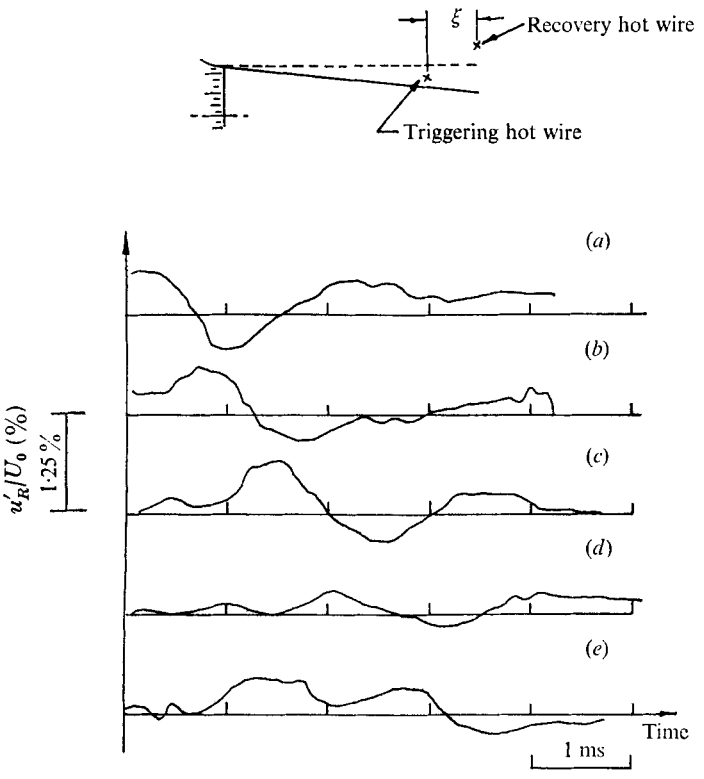

FIGURE 18. Recovered hot-wire signals for $r/D = 0{\cdot}7$. (*a*) $\xi/D = 0$. (*b*) $\xi/D = 0{\cdot}5$. (*c*) $\xi/D = 1{\cdot}0$. (*d*) $\xi/D = 1{\cdot}5$. (*e*) $\xi/D = 2{\cdot}0$.

than expected (e.g. 500 *vs.* about 620 Hz), and the convection velocity tended to be lower also. As will be seen in § 4.7, there appears to be a second flow component in this outer region convecting downstream at a slower speed. It would appear that the recovered signal here is influenced by this second flow component.

Microphone measurements. For completeness, eductions were carried out on the microphone signals in the mixing region. The results are shown in figures 19 (*a*), (*b*) and (*c*), corresponding to eductions at $r/D = 0{\cdot}4$, $0{\cdot}6$ and $0{\cdot}7$ respectively. It may be seen that the curves all have about the same shape, irrespective of whether the recovery probe was at an r/D close to or far from that for the triggering hot wire. Moreover, the curves look more like those in the potential core than corresponding hot-wire curves in the mixing region, in that they decay more slowly than the hot-wire curves. It may also be seen that the corresponding curves of the three figures are in phase with each other and with those of the potential core, consistent with the suggested global nature of the pressure signals. All these characteristics point to the fact that the pressure signals recovered in the mixing region do not come from the localized fluctuations as the hot-wire signals do. From this information, together with the fact that pressure fluctuations in the potential core are results of the passage of the primary vortices alone, the conjecture that the pressure fluctuation everywhere in the flow is mainly influenced by the vortices alone seems well founded.

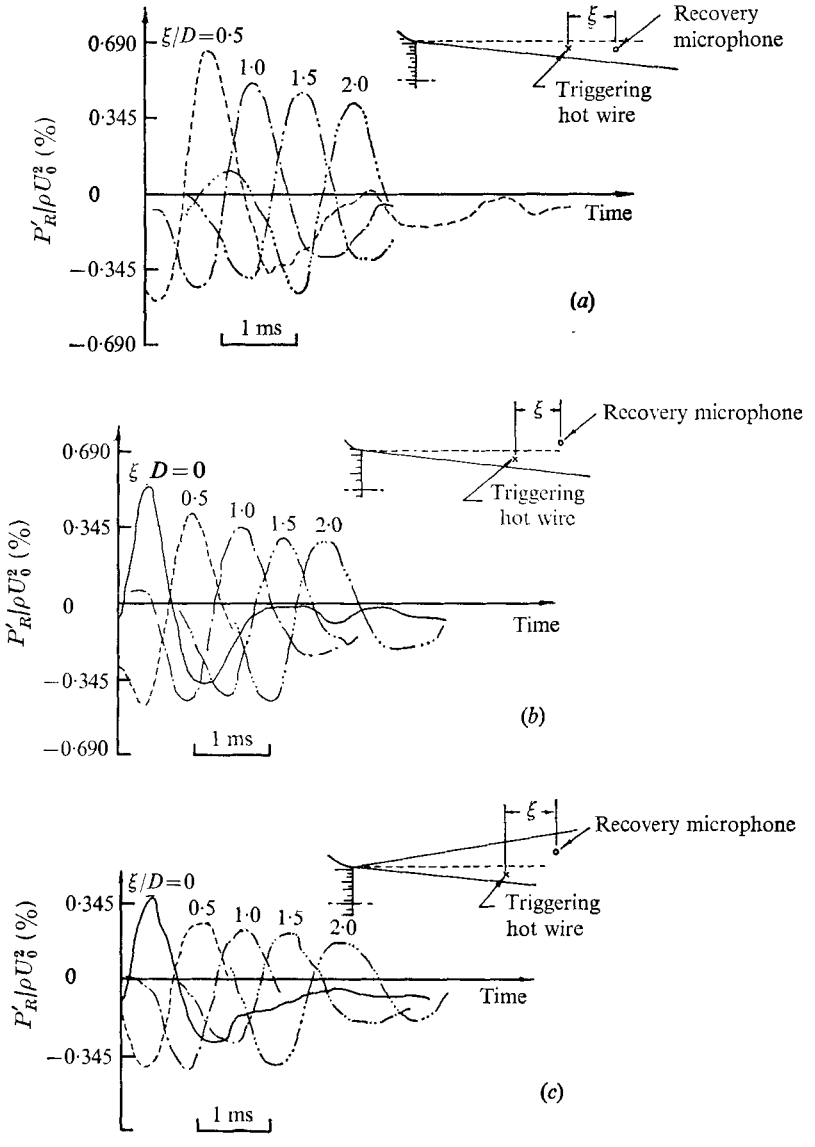

FIGURE 19. Recovered microphone signals for (*a*) $r/D = 0{\cdot}4$, (*b*) $r/D = 0{\cdot}6$ and (*c*) $r/D = 0{\cdot}7$.

The convection velocity and the frequency of oscillation of the curves were determined for each of the cases shown in the figures, and they were found to be about the same as in the potential core.

One other contrasting feature about the pressure curves is that the proportion of the signal recovered remains essentially constant over the whole transverse plane. Reference to curves for the u' fluctuations will show that this is not necessarily the case with hot-wire signals. Therefore, in yet another way, the global nature of the pressure signals is revealed.

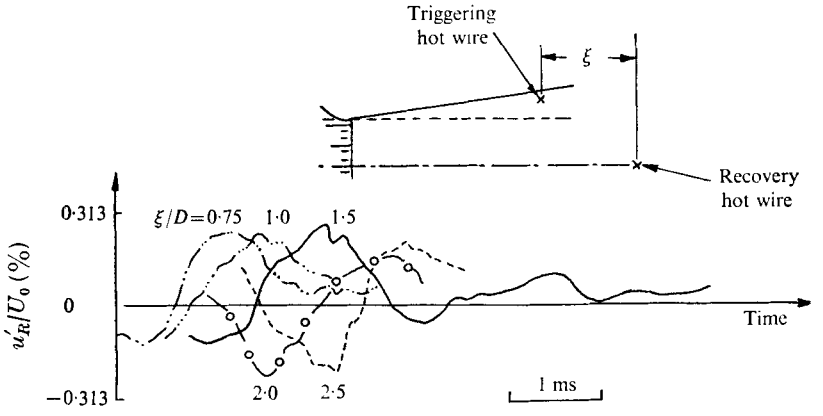

FIGURE 20. Recovered hot-wire signals along jet axis (using upward spikes).

4.7. *Measurements using upward spikes*

In all the earlier results, the eduction was achieved using the downward spikes in the hot-wire signals to initiate it. The downward spikes were found to be fairly regular and have a frequency of occurrence similar to that of the passing vortices. Therefore, they were an obvious choice. It would, however, be of interest to see if one might also successfully educe with the upward spikes as well. For this purpose, the triggering hot wire was moved out to the radial position $r/D = 0{\cdot}7$.

Figure 20 shows the results of eduction along the jets axis triggered this way. It may be seen that the recovered signals are lower than those found earlier using the downward spikes to perform the triggering, and that the curves have a jagged appearance. However, the phase relationships of corresponding curves are maintained and may be seen to be in accordance with the forms predicted from the model. Moreover, an estimate of the convection velocity can be obtained from the curves. This yielded an approximate value of $0{\cdot}68U_0$, the same as was found in the earlier results.

It is clear, therefore, that the upward spikes have some connexion with the passing of the primary vortices. However, the link appears to be weaker in this case than that between the downward spikes and the vortices.

It may be recalled that, during the discussion of the time-history curves in the introduction, some questions were raised regarding the upward spikes since they did not occur at the same frequency as the passing vortices. In fact, it was seen that there appeared roughly to be only one of the large upward spikes for every three downward spikes. However, since each large upward spike appeared to occur at an instant very close to one corresponding to a downward spike and the shape of the spikes appeared to conform with the suggestions of the model, it was speculated that these spikes might be connected with the passing of the vortices. The results above, therefore, confirm this, although the association seems tenuous.

Figure 21 shows the results of another eduction using the upward spikes. For this case, the recovery hot wire was placed directly downstream of the triggering

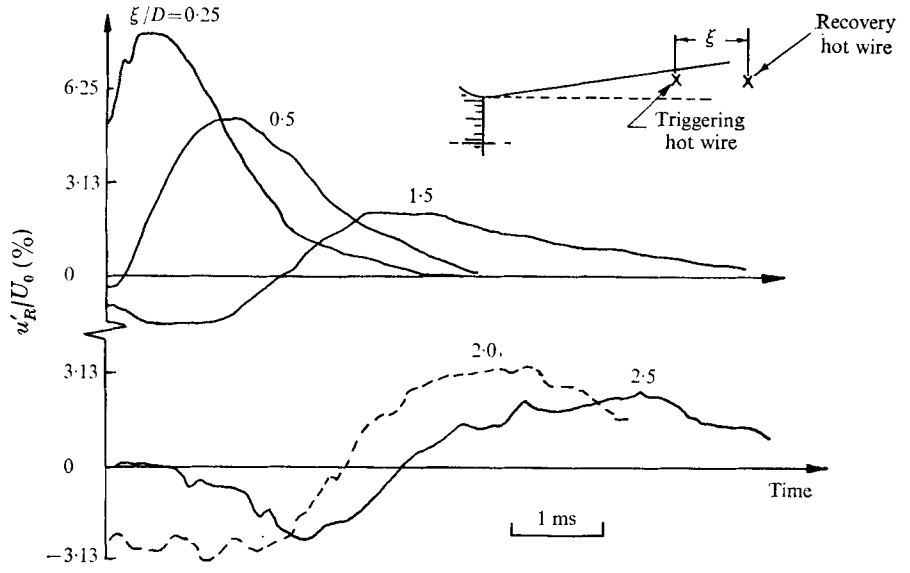

FIGURE 21. Recovered hot-wire signals for $r/D = 0{\cdot}7$ (using upward spikes).

hot wire. It may be seen that the shape of the recovered signals resembles that shown in figure 8 for the outer part of the mixing layer (i.e. $r/D = 0{\cdot}6$ and $0{\cdot}7$) and that the phase relationships are maintained in the correct order. The proportion of the signals recovered was almost as high as unity at this point, and as pointed out earlier, this was possible because of the proximity of the triggering and recovery hot wires.

The convection velocity was determined from the curves of figure 21. Surprisingly, this was found to be $0{\cdot}42U_0$, a value which is substantially lower than those found earlier using the downward spikes to trigger the eduction, or when the upward spikes were used to trigger the eduction of signals in the potential core. Since a meaningful eduction of signals at a position downstream from the triggering hot wire implies that a coherent structure is preserved as it moves downstream, this result must therefore suggest that there is a coherent structure moving downstream on this side of the mixing region at this lower speed. It might thus be speculated that there is a branch from the main vortex street which moves more slowly downstream than the main vortex street.

Thus the following two main results emerge from this subsection.

(i) The upward spikes are in some way associated with the potential-core fluctuations, which may be identified with the vortex street.

(ii) When upward spikes are used to recover signals in the outer part of the mixing region where these spikes are found, a significantly lower convection velocity is obtained, thus indicating the possible existence of a branch of the main vortex street in the entrainment region.

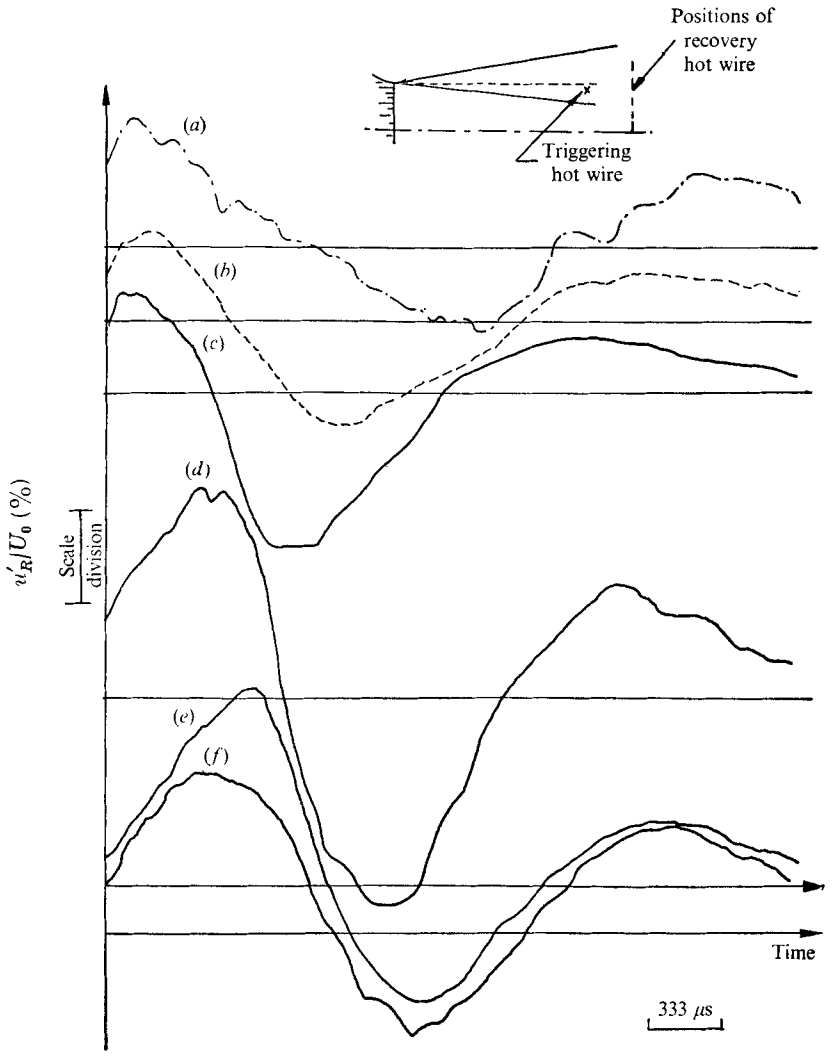

FIGURE 22. Recovered hot-wire signals for $x/D = 2{\cdot}5$.

	(*a*)	(*b*)	(*c*)	(*d*)	(*e*)	(*f*)
Radial position, r/D	0·6	0·5	0·4	0·3	0·2	0
Scale per division (%)	3·13	3·13	0·313	0·625	0·625	0·313

4.8. *Measurements in a transverse plane*

It does seem fairly clear now that a vortex street dominates the structure in a 'turbulent' jet, and that the eduction technique permits extraction of this information. The results obtained using the downward spikes to trigger the eduction were seen generally to confirm the predictions of the postulated model. It would be interesting now to bring some of these results together and consider them from the point of view of what might be experienced at a given transverse plane.

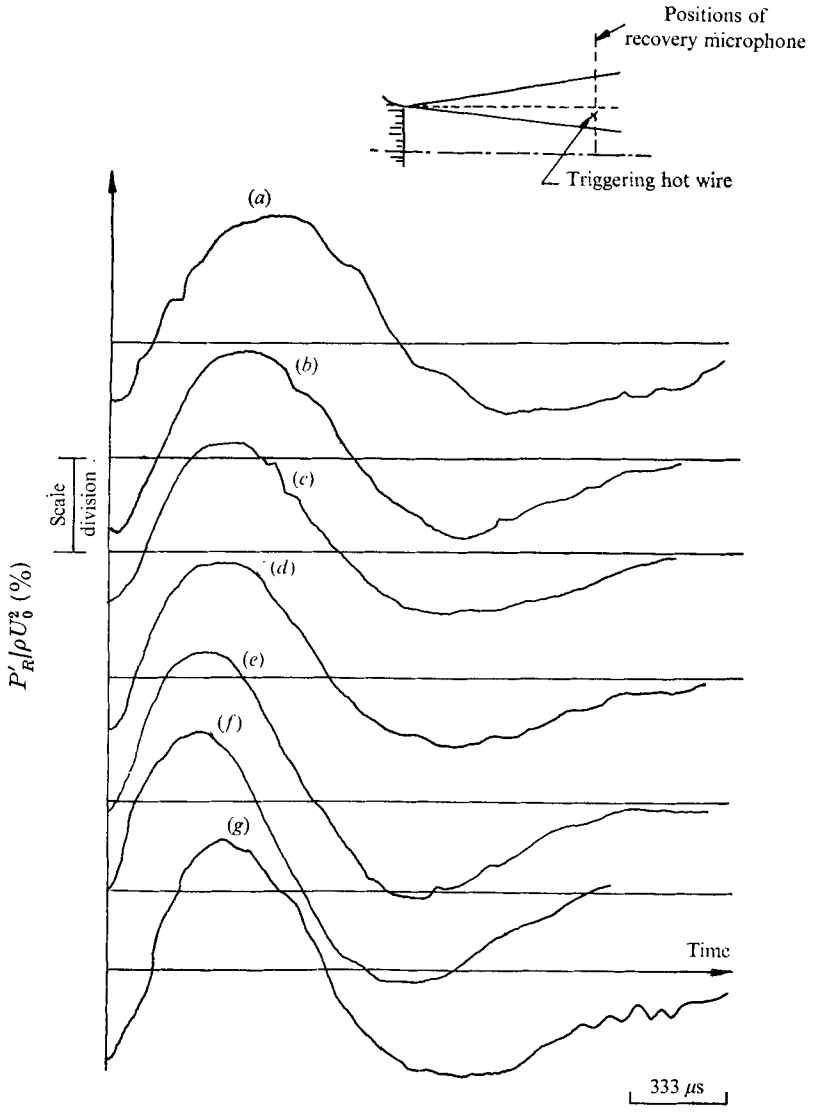

FIGURE 23. Recovered microphone signals for $x/D = 2{\cdot}0$.

	(a)	(b)	(c)	(d)	(e)	(f)	(g)
Radial position, r/D	1·21	0·72	0·62	0·52	0·42	0·33	0
Scale per division (%)	0·022	0·345	0·549	0·549	0·549	0·549	0·172

Phase relationship. Let us first consider the phase relationship of the various results in a transverse plane. Figure 22 shows the recovered u' signals at the station $x/D = 2{\cdot}5$ (i.e. with $\xi/D = 0{\cdot}5$). This station was especially selected for study in order to recover more details about the field surrounding the vortex structure.

It may be seen that when the recovery hot wire is in the potential core, the curves are in phase and have an essentially sinusoidal appearance. However, as

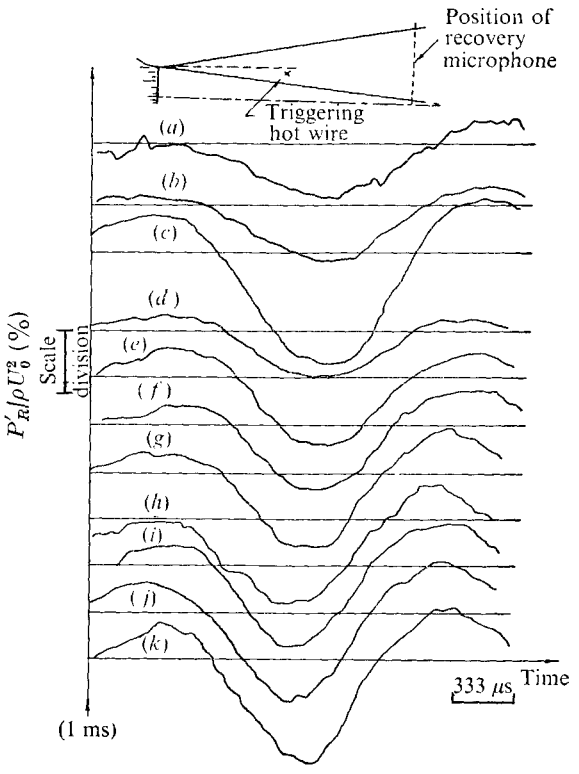

FIGURE 24. Recovered microphone signals for $x/d = 4{\cdot}0$.

	(*a*)	(*b*)	(*c*)	(*d*)	(*e*)	(*f*)	(*g*)	(*h*)	(*i*)	(*j*)	(*k*)
Radial position, R/D	1·21	1·01	0·82	0·72	0·62	0·52	0·42	0·33	0·23	0·13	0
Scale per division (%)	0·22	0·172	0·172	0·549	0·549	0·549	0·549	0·549	0·345	0·345	0·345

the mixing region is entered (from $r/D = 0{\cdot}3$), the curves change their characteristic form and advance in phase. The curves begin to depart from the symmetry of the sinusoidal shape and, instead, appear to show a steeper fall from a positive peak to a negative peak and a more gradual rise to the next positive peak. This agrees exactly with the picture of the field given in figure 7. It may be seen that, when the recovery hot wire is at $r/D = 0{\cdot}4$, the curve appears to be in quadrature with the curves for the potential core. This condition is what one might expect from the postulates of the model. Space–time correlation results also support this (Lau *et al.* 1972).

The curve for $r/D = 0{\cdot}6$ seems to show different behaviour with respect to the spacing of the peaks and the troughs in the curve. It may be seen that the period of time between the first positive peak and the next trough is much longer than that between the trough and the next positive peak. Reference to the bottom curve of figure 7 will show this to be a true representation of what was postulated in the model. A similar comparison of the curve for $r/D = 0{\cdot}4$ with figure 7 (*a*) would also reveal agreement between experimental results and model prediction.

The results for the pressure signals at the transverse plane $x/D = 2{\cdot}0$ (i.e.

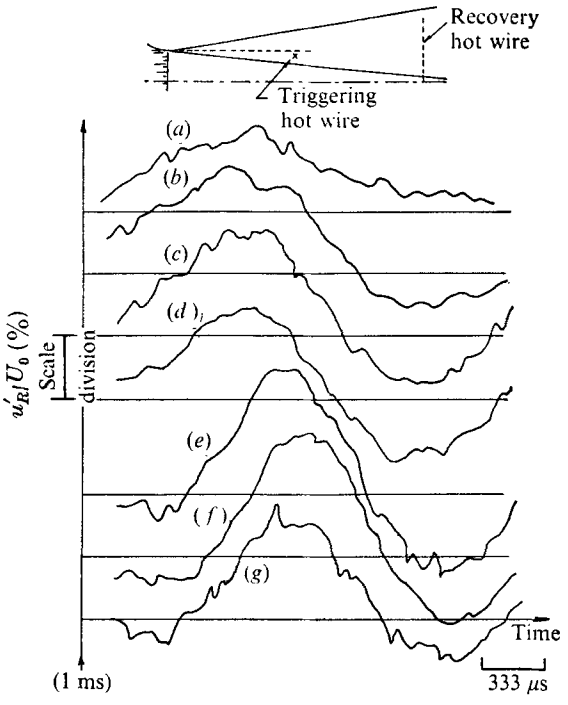

FIGURE 25. Recovered hot-wire signals for $x/d = 4{\cdot}0$.

	(a)	(b)	(c)	(d)	(e)	(f)	(g)
Radial position, r/D	0·6	0·5	0·4	0·3	0·2	0·1	0
Scale per division (%)	1·25	1·25	1·25	1·25	0·625	0·625	0·625

$\xi/D = 0$) are shown in figure 23. It may be seen that all the curves are practically in phase as expected.

To complete the picture, the results for pressure and axial velocity at the axial station $x/D = 4{\cdot}0$ are shown in figures 24 and 25. It may be seen that the observations made above apply equally at this downstream station.

Amplitude of the recovered signals. Figures 26 (*a*) and (*b*) show the radial distributions of the maximum amplitude of the recovered u' and p' signals respectively. They represent results acquired at two axial stations using the hot wire at $x/D = 2{\cdot}0$, $r/D = 0{\cdot}4$ as the trigger probe in each case. The corresponding distributions of r.m.s. values are also shown.

It may be seen that the proportion of the pressure signals recovered remains essentially the same over the whole cross-section. On the other hand, that of the u' signals falls quite substantially in the mixing region. This suggests that in the case of the pressure about the same proportion of the signal is associated with the regular pattern in the mixing region as in the potential core, and lends further support to the concept of a global influence of the pressure. With the u' signals, on the other hand, there appears also to be a localized component in the mixing layer and although this component is framed within the vortex pattern, it is not frozen into the pattern. In the potential core, of course, the proportion of the u' signal recovered is of the same order as that for the p' signals.

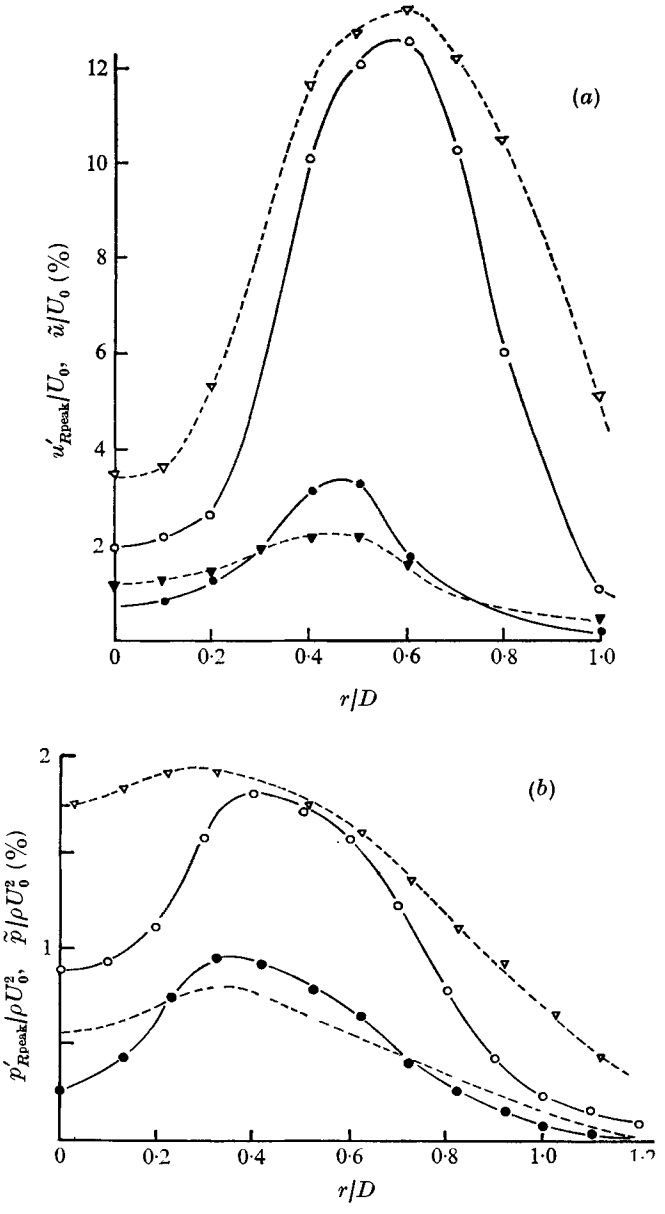

FIGURE 26. Comparison between the amplitudes of (*a*) the u' and (*b*) the microphone signals with their r.m.s. values.

		○	●	▽	▼
(*a*)	Variable	$\tilde{u}/U_0$	$u_{R\text{peak}}/U_0$	$\tilde{u}/U_0$	$u_{R\text{peak}}/U_0$
	x/d	2·5	2·5	4·0	4·0
(*b*)	Variable	$\tilde{p}/\rho U_0^2$	$p_{R\text{peak}}/\rho U_0^2$	$\tilde{p}/\rho U_0^2$	$p_{R\text{peak}}/\rho U_0^2$
	x/d	2·0	2·0	4·0	4·0

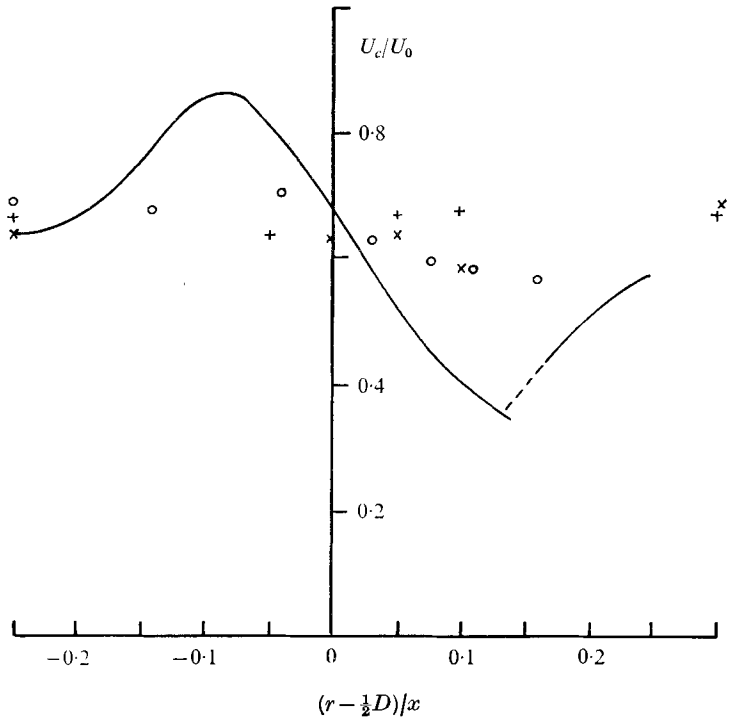

FIGURE 27. Radial distribution of convection velocity. ○, p', u' correlation; ×, u' eduction; +, p' eduction; ---, u', u' correlation.

Convection velocity. It was found (Lau 1971) that the convection velocity of signals associated with pressure fluctuations tended to be constant over a cross-sectional plane. This result was determined from correlation measurements. It was found that the v' signals on the inner side of the jet appeared to behave in the same way. The only outstanding signals which gave substantial deviations from this constant value were seen to be the u' signals. It was then suggested that the more global components of fluctuations would tend to be convected with the same speed throughout a given cross-section.

Convection velocities of the various component fluctuations were also determined from the results of the educed signals. It was seen that irrespective of whether the u' or p' signals were considered a constant value of the convection velocity was found over the transverse plane.

These results are summarized in figure 27, in which the results from the eduction technique are shown as crosses. It may be seen in fact that the convection velocities obtained by this technique have a consistently even value. It is clear that the technique allows the recovery of the components of the fluctuations associated with the vortices irrespective of the actual fluctuating component being measured. The uniformity in the convection velocity obtained in a transverse plane by the eduction technique would therefore also lend support to the proposed model.

4.9. *Vortex core radius*

Since the phase relationships with respect to the vortices of the model seem to be very well reproduced in the results of the educed signals, it should be possible to obtain an order-of-magnitude assessment of the vortex core radius.

It was pointed out in the discussion of figure 7 that pressure fluctuations would show a trough whenever the centre of the vortex passed the observer. This phase relationship appears to be fairly well borne out in the earlier results of this section. The pressure appears to have a global influence, and the curves of recovered pressure signals (figures 23 and 24) have well-defined peaks.

Now, if it is assumed that (i) the origins of the curves represent the average instants when the spikes in the u' signals trigger the eduction, (ii) the peaks of the spikes locate the approximate extent of the vortex core, and (iii) the troughs in the pressure curves represent the positions of a vortex centre, it should be possible to estimate the time interval between the instant when the vortex centre passed and the instant when the edge of the vortex core passed. Applying this method to the results shown by the bottom curve of figure 23, this time interval was found to be about $140\,\mu$s. Since the convection velocity is about $0{\cdot}65U_0$, an average distance between the spikes and the associated vortex centres is estimated to be $0{\cdot}1D$.

In actual fact, it is expected that this distance will be greater than the vortex core radius in view of the fact that the trailing edge of the vortex causing the spikes probably trails to the next vortex behind it as shown in figure 1.

This effort will have to be extended before a definite value of the vortex core radius can be obtained. However, on the basis of the present data it would seem that at an axial position of $x/D = 2{\cdot}0$ the vortex core radius would most probably be less than $0{\cdot}1D$.

5. Conclusion

From the results of this investigation, it does appear that a significant portion of the 'turbulent' jet flow structure within the first few diameters is in fact relatively simple. The main body of the flow seems to be built around a structure consisting of an axial array of vortices, spaced about one and a quarter diameters apart.

As reported previously (Lau *et al.* 1972) it appears that the induced fields of these vortices account for fluctuations observed in the jet potential core and entrainment region. However, in the jet mixing layer an additional mechanism is required to account, in particular, for the existence of a mean Reynolds shear stress. It is suggested that the leading edge of each vortex induces a transfer of high velocity fluid to the low speed side of the mixing layer, while the trailing edge causes the transfer of low velocity fluid towards the jet potential core. Qualitatively, this is shown to account for both the Reynolds shear stress and for the observed 'spikey' nature of the signals observed, in particular, on the potential-core side of the mixing layer.

In this study, particular interest was taken in the mechanism by which these

spikes in the u' signals were generated in the mixing region. The proposed model was found to give an adequate description of the mechanism for the spikes, and it was shown statistically that the downward spikes did indeed have a high probability of occurring at the same frequency as the proposed vortex passing frequency, thus identifying them with the passing vortices as the model suggests. However, the probability distribution was seen to be spread over a large range of frequencies. This suggested that perhaps the vortices were not as regular and orderly as was ideally assumed, and that the method of time-domain averaging (eduction) would be useful for revealing the basic structure of the flow surrounding the vortices.

The spikes were used to trigger the eduction process. It was found that the curves of the educed signals were of the same shape and possessed the same phase relationships as was predicted by the extended model. In particular, it was found that the spikes in the u' signals could be recovered and that their shapes followed the predictions of the model closely. It would seem therefore that the recovered u' signals in the mixing layer are closely associated with the cross-flow induced by the vortices in this region. It appears also that this secondary flow attempts to preserve its phase relationships with the main body of the vortices as they move downstream together.

The pressure was found to have a global influence, and from the phase relationships exhibited by the recovered signal it would appear that the signal predominantly came from the primary vortices alone (i.e. the cross-flow had little influence on pressure results).

The vortices appear to move downstream at a fairly consistent speed. This was seen by the fact that meaningful signals could be recovered even at the positions downstream from the triggering hot wire provided that they were associated with the vortices directly involved with the triggering process. The vortices, however, appear to be less consistently spaced, as only about one and a half wavelengths of the signal were significantly recovered, i.e. only the portion of the signal directly associated with the triggering vortex could be prominently recovered.

The amplitude of signals recovered was found generally to be about one-quarter of the r.m.s. value of the corresponding overall signal in the potential core. This low proportion of signal recovered is probably due to the inconsistencies of the triggering spikes and the possibility that the successive eductions were not triggered at the same instant relative to the vortex centres. It might also be due to the signals themselves not being fully repeatable, just as oscilloscope traces have already indicated.

The proportion of u' signals in the mixing region recovered was found to be generally much lower than the norm except when the recovery hot wire was very close to the triggering hot wire. This may be taken to suggest that the cross-flows are not 'frozen' onto the vortices.

The upward spikes in the outer region were also used to educe signals in the field. It appears from the results that the upward spikes have some connexion with the primary vortices of the model but that the connexion is not as strong as with the downward spikes. It was suggested that a second component might be influencing the flow in this outer region and affecting the results here. This will

be a subject for consideration in part 2. In the present results, however, the large upward spikes have shapes which seem to follow the edicts of the vortex model.

To sum up, therefore, the model appears to give a reliable picture of the flow structure in the jet. There are still some obstacles to a full understanding of the flow structure with respect to the flow on the entrainment side of the mixing region. However, by and large it seems fairly well established that the dominant structure in the first few diameters of a round jet consists of an axial array of possibly toroidal vortices convecting downstream, and as these vortices move downstream they sweep fluid from the high velocity side of the jet to the other and vice versa.

The authors wish to thank the National Gas Turbine Establishment, England, for their financial support of this work, which was completed in 1971 whilst the first author was a research fellow at the Institute of Sound and Vibration Research, University of Southampton. Since 1971 these studies have been extended at the I.S.V.R. by an independent group of workers under the supervision of Professor P. O. A. L. Davies. A summary of their work has recently been presented in *I.S.V.R. Memo*, no. 506 (1974).

REFERENCES

ANDERSON, A. B. C. 1956 *J. Acoust. Soc. Am.* **28**, 914.

BRADSHAW, P., FERRISS, D. H. & JOHNSON, R. E. 1964 *J. Fluid Mech.* **19**, 591.

DAVIES, P. O. A. L., FISHER, M. J. & BARRATT, M. J. 1963 *J. Fluid Mech.* **15**, 337.

DAVIES, P. O. A. L., KO, N. W. M. & BOSE, B. 1968 *Aero. Res. Counc. Current Paper*, no. 989.

FRANKLIN, R. E. & FOXWELL, J. H. 1960 *Aero. Res. Counc. R. & M.* nos. 3161, 3162.

FUCHS, H. V. 1970 *Dsch. Luft- & Raumfahrt Rep.* DLR-FB 70-22.

KO, N. M. W. & DAVIES, P. O. A. L. 1971 *J. Fluid Mech.* **50**, 49.

LAU, J. C. 1971 Ph.D. thesis, I.S.V.R., University of Southampton.

LAU, J. C., FISHER, M. J. & FUCHS, H. V. 1972 *J. Sound & Vib.* **22**, 379.